Available online at www.sciencedirect.com
SCIENCE DIRECT®
Coordination Chemistry Reviews 248 (2004) 351–375
COORDINATION CHEMISTRY REVIEWS
www.elsevier.com/locate/ccr

Review

Structure and bonding in metal sulfoxide complexes: an update

Mario Calligaris*

Dipartimento di Scienze Chimiche, Università di Trieste, 34127 Trieste, Italy

Received 9 October 2003; accepted 10 February 2004

Contents

Abstract

Average S–O bond distances were calculated, from accurate X-ray data, for free and coordinated sulfoxides, showing a decrease from free sulfoxides (avearge 1.492(1) Å) to S-bonded metal complexes (average 1.4738(7) Å). On the contrary, the S–O bond distance increases in H-bonded uncoordinated sulfoxides (S–O···H, average 1.513(2) Å), and more markedly in O-bonded metal complexes (average 1.528(1) Å). Longer S–O bond lengths are found in the $[(\text{sulfoxide–O})_2\text{H}]^+$ (average 1.541(3) Å) and $[(\text{sulfoxide–O})\text{H}]^+$ cations (average 1.587(2) Å). This trend is consistent with that of the SO stretching frequencies, and is definitely supported by quantum chemical calculations for dmso, $[(\text{dmso})\text{H}]^+$, and platinum and ruthenium dmso complexes. DFT quantum chemical investigations about linkage isomerism and isomer

Abbreviations: acv, 9-(2-hydroxyethoxymethyl)guanine; bbso, *n*-butyl-*t*-butyl sulfoxide; bese, 1,2-bis(ethylsulfinyl)ethane; bmse, 1,2-bis(methylsulfinyl)ethane; bmso, *t*-butylmethyl sulfoxide; bpse, 1,2-bis(phenylsulfinyl)ethane; bpsp, 1,3-bis(*n*-propylsulfinyl)propane; btsh, 3,4-bis(*p*-tolylsulfinyl)hexane; btse, 1,2-bis(*p*-tolylsulfinyl)ethane; dbso, di-*n*-butyl sulfoxide; dmim, 1,2-dimethylimidazole; dmpo, 2,8-dimethylphenoxathiin 10-oxide; dmpy, 3,5-dimethylpyridine; dmtsea, *N*,*N*-dimethyl-2-(*p*-tolylsulfinyl)ethylamine; dmso, dimethyl sulfoxide; dmsso, dimesityl sulfoxide; dpso, diphenyl sulfoxide; mpso, methylphenyl sulfoxide; noso, $[(C_6H_4)\text{N(H)C(O)C(OH)C}(p\text{-tolyl})]\text{SO}$; pdtdo, 2-phenyl-1,3-dithiane *trans*-1, *trans*-3-dioxide; ppso, $[(CH_2)_3\text{S}(CH_2)_2\text{P(Ph)}\ (CH)_2\text{S}(CH_2)_3]\text{SO}$; psp, 2-(phenylsulfinyl)propionate; ptaso, $[(C_{11}H_{14}F_3NO_2)\ (CH_2)\ (p\text{-tolyl})]\text{SO}$; tbsa, *t*-butylsulfinylacetate; tmbim, 1,5,6-trimethylbenzimidazole; tmem, *N*,*N*,*N*′,*N*′-tetramethylethylenediamine; tmso, tetramethylene sulfoxide

* Tel.: +39-040-676-3933; fax: +39-040-676-3903.
E-mail address: calligaris@univ.trieste.it (M. Calligaris).

doi:10.1016/j.ccr.2004.02.005

equilibration are also reported and discussed with reference to the experimental evidence. Finally, the stereochemistry of ruthenium sulfoxide complexes is discussed on the basis of molecular mechanics calculations, showing the role of intramolecular steric interactions.

Keywords: Sulfoxides; Metal complexes; Structure; IR data; Quantum-chemical calculations; Conformational analysis

1. Introduction

In the recent past, the coordination chemistry of sulfoxides has been the subject of several review articles, focussing on various reactivity and stereochemistry features of metal complexes [1–5]. Recently, a thorough review concerning the use of transition metal dmso complexes as precursors in inorganic synthesis was prepared by Alessio [6]. However, to the best of the author's knowledge, there is no review concerning the quantum chemical studies on coordination dmso compounds, which appear of interest to provide a theoretical basis for the numerous experimental observations.

The scope of this paper is that of presenting the results of such studies, with particular emphasis on the metal–dmso bonding and S/O linkage isomer equilibria. IR spectra are also discussed, as well as empirical force field investigations of stereochemical features in mono- and di-sulfoxide metal complexes. Finally, the trend of the calculated S–O bond lengths, passing from 'free' to metal bound sulfoxide ligands, is also discussed, in connection with the experimental IR spectroscopy and X-ray diffraction data. In fact, in spite of the wealth of structural data now available, there seems to be no general agreement about the variation, with respect to uncoordinated sulfoxides, of the S–O bond distance upon O-coordination [7], while it is fully recognized that the S–O bond length is shortened upon S-coordination. This uncertainty derives from the fact that some authors assume the distance of 1.513(5) Å, found crystallographically for pure dmso at 5 °C, as the reference value, while others (including the author) believe that this value is not correct, mainly because of the poor quality of the diffraction intensities from the dmso low melting crystals (dmso, mp 18.45 °C). In fact, in this structural determination that dates back to 1966, 35% of the data were 'unobserved' preventing an accurate structure refinement ($R = 7.4\%$, $R_w = 10.3\%$) [8]. It has been suggested that the mean value of 1.492(1) Å, obtained by averaging a large number of accurate dmso–solvate and other pure sulfoxide structures, represents a good estimate for the 'true' value of the S–O bond distance in free dmso [4,5]. In order to enhance the statistical meaning of the means, new data were taken into account and the results are discussed on the basis of various statistical parameters.

For convenience, the oberved data will be presented first.

2. Stereochemical features

The structural aspects examined here are restricted to the metal–sulfoxide linkage, and therefore they refer to the analysis of the observed S–O bond lengths and stretching frequencies. The different sulfoxide bonding modes are also discussed, with particular attention to the sulfoxide bridging ability.

2.1. X-ray structures

A recent statistical analysis of the structural parameters of uncoordinated sulfoxides and of their O- and S-coordinated metal complexes had shown that the average S–O bond distances are, respectively, of 1.492(1) (free), 1.527(1) (O-bonded), and 1.4719(8) Å (S-bonded) [5], in perfect agreement with the values reported previously [4]. The available data also indicated that the S–O bond length slightly increases, both in free and coordinated sulfoxides, when the oxygen atom is involved in hydrogen bonding [4,5], while a marked lengthening was observed in the case of sulfoxide protonation.

In order to confirm the trends above, new literature data were included, as reported below. The results are then discussed in Section 2.1.4.2.

2.1.1. Uncoordinated sulfoxides

Sulfoxides whose structural parameters were not included in the previous surveys [4,5] are reported below, separately, for acyclic, cyclic, and H-bonded sulfoxides, with S–O bond distances in brackets.

Acyclic: dmso (solvate, 1.494(6) Å [9], 1.506(1) Å [10]); tbsa (1.487(3) Å [11]; dpso (1.492(1) Å [12], 1.495(1) Å [13]]; dmsso (1.484(2) Å [14]); ptaso (1.479(5) Å [15]); btse (1.487(1), 1.492(1) Å [16]); bpsp (1.490(7), 1.483(7) Å [17]).

Cyclic: dmpo (1.499(2), 1.503(3) Å [18]); ppso (1.53(1), 1.47(1) Å [19]); noso (1.495(3) Å [20]).

H-bonded: dmso (1.494(5) Å [21], 1.504(2) Å [22], 1.514(1) [23], 1.515(1) Å [24], 1.517(1) [25], 1.519(1) Å [26], 1.538(3) Å [27]).

2.1.2. Protonated sulfoxides

In the solid state, protonation of the oxygen atom of dmso was first shown by B. R. James et al. in the rhodium complex $[(dmso)_2H][RhCl_4(dmso)_2]$. In fact, the O···O distance of 2.420(5) Å in the cation clearly showed the formation of a very strong hydrogen bond between the two dmso O atoms sharing the hydrogen ion [28]. Later, this binding mode was confirmed by several other structure determinations exhibiting a 'symmetric' H-bond [4,5]. In $[(dmso)_2H](TeCl_6)\cdot 2dmso$, the H atom was localized, on difference Fourier maps, close to one of the two oygen atoms showing the formation of the $[Me_2SO–H^+\cdots OSMe_2]$

cation [29]. This is in agreement with the two different S−O bond lengths, 1.585(8) Å in Me_2SO–H^+ and 1.529(8) Å in the hydrogen-bonded dmso molecule. In the case of tmso, a $[(tmso)H]^+$ cation was found in $[(tmso)H][RuCl_4(tmso)_2]$, whose difference electron density map definitely showed tmso protonation on the O atom, that caused a marked lengthening of the S–O distance up to 1.589(3) Å [30].

Recent structural data for protonated sulfoxides refer to dmso ($[(dmso)_2H]^+$, 1.50(2), 1.53(2) Å [31]), and tmso ($[(tmso)_2H]^+$, 1.542(4) Å [32]).

2.1.3. Metal sulfoxide complexes

Metal sulfoxide complexes (S–, O–, and μ–S,O bonded) whose structural parameters were not included in the previous surveys [4,5] are reported below, separated into groups, with indication of the metal atom and the sulfoxide ligand.

2.1.3.1. S-bonded complexes.

Group 8: Ru(II)–dmso [33–53]; Ru(II)–mpso [54]; Ru(II)–psp [55]; Ru(III)–dmso [56–62]; Os(II)–dmso (38, 63); Os(II)–psp [55].

Group 9: Rh(I)–dmso [64]; Rh(I)–btse [16]; Rh(II)–dmso [65]; Rh(III)–dmso [66]; Rh(III)–psp [55]; Ir(I)–dmso [67]; Ir(I)–btse [16]; Ir(III)–dmso [31,66,67]; Ir(III)–psp [55].

Group 10: Pd(II)–dmso [68]; Pd(II)–dmtsea, Pd(II)–btsh [69]; Pd(II)–btse [16]; Pt(II)–dmso [70–78]; Pt(II)–btse [16].

2.1.3.2. O-bonded complexes.

Group 3: Y(III)–dmso [79]; Gd(III)–dmso [80]; U(IV)–dmso [81]; U(VI)–dmso [82].

Group 7: Mn(II)–dmso [83]; Re(I)–bmso [84].

Group 8: Fe(III)–dmso [85]; Ru(II)–dmso [86]; Ru(III)–dmso [58]; Ru(III)–tmso [32].

Group 9: Co(III)–dmso [87]; Rh(I)–dmso [64]; Rh(II)–dmso [7]; Ir(III)–dmso [67].

Group 10: Ni(II)–dmso [10]; Pd(II)–dmso [88]

Group 11: Cu(II)–dmso [89]; Cu(II)–bmse; Cu(II)–bpsp [17].

Group 12: Zn(II)–dmso [90]; Hg(II)–bbso [91]

Group 14: Ge(IV)–dmso [92]; Sn(IV)–dmso [93,94]; Sn(IV)–pdtdo [95].

2.1.3.3. μ–S,O complexes.

Group 8: Ru(II)–mpso [54].

Group 9: Rh(I)–dmso [64]; Rh(II)–dmso [7].

2.1.4. Average molecular dimensions

2.1.4.1. Treatment of data. It has been proposed [96] that the best estimate of the average molecular dimensions from crystallographic data is provided by the weighted mean ($\langle x\rangle_w$) when environmental (e.g. crystal packing) effects are negligible. On the contrary, when environmental effects are large compared with experimental errors, the unweighted mean ($\langle x\rangle_u$) represents the best estimate of the mean [96]. In intermediate cases, the 'semi-weighted' mean ($\langle x\rangle_s$) is more appropriate [96]. Considering a sample of n observations, x_i, the three means are defined as: $\langle x\rangle_u = \sum_i x_i/n$, $\langle x\rangle_w = \sum_i w_i x_i/\sum_i w_i$, and $\langle x\rangle_s = \sum_i W_i x_i/\sum_i W_i$, respectively. The weights (w_i) and 'semi-weights' (W_i) are: $w_i = 1/\sigma^2(x_i)$ ($\sigma(x_i)$ is the individual estimated standard deviation from least-squares refinements), and $W_i = 1/[\sigma^2(x_i) + \sigma^2(\mu)]$, with $\sigma^2(\mu) = \sigma^2 - \Sigma_i[\sigma^2(x_i)]/n$, in which σ is the sample standard deviation, given by $[\Sigma_i(x_i - \langle x\rangle_u)^2/(n-1)]^{1/2}$. The standard errors of the three means are calculated as: $\sigma(\langle x\rangle_u) = \{\Sigma_i(x_i - \langle x\rangle_u)^2/[n(n-1)]\}^{1/2}$, $\sigma(\langle x\rangle_w) = (\Sigma_i w_i)^{-1/2}$, and $\sigma(\langle x\rangle_s) = (\Sigma_i W_i)^{-1/2}$, respectively.

As in the previous statistical analyses of the structural parameters of uncoordinated and coordinated sulfoxides [4,5], only sufficiently accurate data were used (ordered structures, with estimated standard deviations less than 0.015 Å for bond lengths, and less than 1.5° for bond angles). Furthermore, the individual $\sigma(x_i)$ values were multiplied by 1.3, to take into account the usual underestimation of the experimental errors derived from least-squares refinement methods [96].

Merging the present observations with those previously considered [5], we obtain the values reported in Tables 1–6. In Tables 1, 2, 5 and 6, besides the above parameters, also the minimum and maximum values, the median (m), the upper (q_u) and lower (q_l) quartiles, the skewness (defined as $\{\Sigma[(x_i - \langle x\rangle_u)/\sigma)]^3\}/n$, and the 98% confidence interval for the mean ($C_{0.98}$) [97a] are given. For small samples ($n < 30$), a correction to $C_{0.98}$ was applied according to the Student's t-distribution [97b]. In Tables 3 and 4, when the

Table 1
Statistics of bond lengths (Å) and angles (°) in uncoordinated sulfoxides

	S–O[a]	S–C(sp^3)[b]	C–S–C[b]	O–S–C[b]
Minimum	1.460	1.730	92.2	101.0
Maximum	1.528	1.858	103.5	113.3
n	119	116	87	175
Median	1.493	1.794	98.0	106.0
q_l	1.486	1.778	97.0	104.9
q_u	1.498	1.813	98.5	106.9
σ	0.0104	0.0265	1.61	1.59
$\langle\sigma_i\rangle$	0.0045	0.0057	0.32	0.31
Skewness	–0.038	0.064	–0.059	0.253
$\langle x\rangle_u$	1.4922	1.7949	97.84	105.97
$\sigma(\langle x\rangle_u)$	0.0010	0.0025	0.17	0.12
$\langle x\rangle_s$	1.4919	1.7955	97.78	105.98
$\sigma(\langle x\rangle_s)$	0.0011	0.0026	0.18	0.12
$\langle x\rangle_w$	1.4924	1.8005	97.66	105.87
$\sigma(\langle x\rangle_w)$	0.0003	0.0005	0.02	0.02
$C_{0.98}$	±0.0022	±0.0057	±0.40	±0.28

[a] Cyclic sulfoxides included.
[b] Cyclic sulfoxides excluded.

Table 2
Statistics of S–O bond lengths (Å) in uncoordinated sulfoxides involved in hydrogen-bonded and in $[(\text{sulfoxide–O})_2\text{H}]^+$ protonated species

S–O	Sulfoxide–O···H–	$[(\text{Sulfoxide–O})_2\text{H}]^+$
Minimum	1.494	1.528
Maximum	1.538	1.559
n	27	12
Median	1.512	1.538
q_l	1.505	1.536
q_u	1.518	1.548
σ	0.0096	0.0086
$\langle\sigma_i\rangle$	0.0040	0.0037
Skewness	0.43	0.69
$\langle x\rangle_u$	1.5131	1.5402
$\sigma(\langle x\rangle_u)$	0.0018	0.0025
$\langle x\rangle_s$	1.5131	1.5407
$\sigma(\langle x\rangle_s)$	0.0021	0.0028
$\langle x\rangle_w$	1.5123	1.5438
$\sigma(\langle x\rangle_w)$	0.0005	0.0011
$C_{0.98}$	±0.0046	±0.0068

semi-weighted mean cannot be calculated, the mean with the highest standard error is reported. Normality tests were applied using the graphical *rankit* procedure [97c] and the χ^2 test [97d].

2.1.4.2. S–O mean bond lengths. The distributions of the structural parameters reported in Tables 1 and 2 for uncoordinated sulfoxides are found, by both the *rankit* and the χ^2 tests, to be, with good approximation, normal. They are also nearly symmetrical, with the exception of the S–O distances in the $[(\text{sulfoxide–O})_2\text{H}]^+$ ions. In all cases, the unweighted and semi-weighted means are close, as well as their standard errors, suggesting that the variance is essentially determined by environmental effects rather than by the experimental errors [96]. Inspection of these Tables shows that the average S–O bond length increases from free sulfoxides to H-bonded and protonated species. Rounding the values at the last significant digit, the $\langle x\rangle_s$ values with their 98% confidence intervals are: 1.492 ± 0.002 Å (free sulfoxides),

Table 3
Average dimensions for O-bonded metal sulfoxide complexes

Group	M	M–O	S–O	S–C	M–O–S	O–S–C	C–S–C
1	Na(I)	2.31(2) 0.05 [4]	1.52(1) 0.02 [3]	1.76(2) 0.04 [3]	131(11) 20 [3]	104(2) 3 [4]	98(1) 1 [2]
3	Y(III)	2.30(3) 0.05 [3]	1.512(5) 0.006 [2]	1.754(8) 0.01 [4]	136(5) 7 [2]	105(2) 2 [2]	99(1) 1 [2]
	Ln(III)[a]	2.38(1) 0.06 [27]	1.512(2) 0.009 [27]	1.786(3) 0. 02 [36]	143(3) 11 [20]	104.9(2) 1 [39]	98.6(3) 1 [20]
	U(IV)	2.36(1) 0.03 [7]	1.540(2) 0.005 [7]	1.776(2) 0.006 [14]	134(2) 6 [7]	104.2(3) 1 [14]	100(2) 6 [16]
	U(VI)	2.382(9) 0.028 [10]	1.525(6) 0.015 [10]	1.787(8) 0.03 [16]	131(2) 7 [10]	105.4(8) 4 [20]	101(2) 7 [10]
4	Ti(IV)	2.11(1) 0.06 [17]	1.527(3)[b] 0.010 [16]	1.774(5) 0.013 [11]	122.6(9) 4 [16]	104.1(3) 1 [32]	98.3(4) 1 [16]
	Zr(IV)	2.202(5) 0.013 [7]	1.539(2) 0.005 [7]	1.778(2)[a] 0.007 [14]	127.3(7) 2 [6]	104.3(5) 2 [14]	98.8(5) 1 [7]
5	V(IV)[c]	2.04[b] 0.01	1.52[b] 0.02	1.80[b] 0.01	125[b] 1	104[b] 2	98.8[b] 0.7
6	Cr(III)	1.981(8) 0.017 [5]	1.538(7) 0.015 [5]	1.774(5) 0.01 [10]	127.4(6) 1 [5]	103.4(6) 2 [10]	98.6(4) 0.8 [5]
	Mo(II)	2.134(8) 0.009 [2]	1.521(5)[d] 0.004 [2]	1.767(7) 0.01 [4]	130(1) 2 [2]	103.6(5) 0.9 [4]	99.9(4)[b] 0.6 [2]
	Mo(VI)	2.27(2) 0.06 [8]	1.523(4) 0.009 [8]	1.776(7) 0.02 [11]	125(2) 5 [8]	104.5(4) 1 [16]	98.7(3) 0.7 [7]
7	Mn(II)	2.160(8) 0.020 [8]	1.511(5) 0.011 [8]	1.776(8) 0.03 [16]	128(3) 9 [8]	105.4(4) 1 [15]	99.1(6) 2 [8]
	Re(I)	2.122(5)[e]	1.558(5)[e]	1.81(3) 0.04 [2]	115.0(3)[e]	103(1) 2 [2]	103.4(5)[e]
	Re(III)	2.302(6)[e]	1.540(6)[e]	1.80(1) 0.02 [2]	129.7(4)[e]		
8	Fe(0)	2.064(9)[e]	1.528(8)[e]	1.797(9)[e]	109.9(4)[e,f]	100.6(4)[f]	90.3(6)[e,f]
	Fe(II)	2.13(1) 0.01 [3]	1.525(7) 0.012 [3]	1.786(5) 0.01 [6]	122(1) 2 [3]	104.3(6) 2 [8]	98.4(2)[b] 0.4 [3]

Table 3 (*Continued*)

Group	M	M–O	S–O	S–C	M–O–S	O–S–C	C–S–C
	Fe(III)	2.05(2) 0.04 [4]	1.529(6) 0.011 [4]	1.80(2) 0.06 [6]	125(1) 2 [4]	104.6(7) 2 [6]	98.5(9) 2 [3]
	Ru(II)	2.10(1) 0.05 [21]	1.545(3) 0.013 [21]	1.783(5) 0.012 [35]	122.0(7) 3 [21]	103.8(5) 3 [42]	99.2(3) 1 [21]
	Ru(III)	2.088(9) 0.033 [14]	1.540(5) 0.017 [14]	1.783(5) 0.026 [26]	121.5(7) 3 [14]	103.1(3) 1 [17]	99.4(5) 2 [11]
	Os(III)	2.08(5) 0.06 [2]	1.54(3) 0.04 [2]	1.775(3)[b] 0.007 [4]	123.55(5)[b] 0.07 [2]	103.0(5) 0.8 [4]	99.8(3)[b] 0.6 [3]
9	Co(II)	2.084(7) 0.014 [7]	1.52(1) 0.03 [7]	1.80(2) 0.07 [16]	121(1) 4 [8]	104(1) 4 [16]	98(2) 6 [7]
	Co(III)	1.94(1) 0.02 [3]	1.537(9) 0.015 [3]	1.776(5) 0.008 [4]	129(4) 7 [3]	103.3(8) 2 [6]	99.7(2)[b] 0.3 [3]
	Rh(II)[g]	2.238(9) 0.019 [6]	1.51(2) 0.02 [2]	1.80(3) 0.04 [2]	132.4(2)[e]	105.9(3)[b] 0.7 [4]	97.9(6)[b] 0.9 [2]
	Rh(III)	2.06(2) 0.04 [4]	1.549(2)[f] 0.003 [3]	1.769(5) 0.009 [6]	121(1) 2 [4]	103.6(6) 2 [11]	99.0(4)[b] 0.7 [4]
10	Ni(II)	2.11(3) 0.08 [6]	1.524(4) 0.008 [6]	1.779(4) 0.01 [10]	121(2) 4 [5]	104.6(4) 1 [12]	98.1(3) 0.7 [6]
	Pd(II)	2.08(2) 0.05 [7]	1.537(7) 0.017 [7]	1.784(6) 0.02 [9]	121(1) 4 [7]	103.3(4) 1 [14]	99.3(3)[b] 0.9 [7]
	Pt(II)	2.046(9)[d] 0.008 [2]	1.55(2) 0.02 [2]	1.78(1)[d] 0.01 [4]	122(1) 2 [2]	103.0(9) 1 [4]	99.0(8)[d] 0.9 [2]
11	Cu(I)	2.223(3)[e]	1.57(6)[e]	1.6(2)[e]	117(2)[e]	104(4)[e]	97(2)[e]
	Cu(II)	2.03(2) 0.14 [46]	1.523(4) 0.021 [40]	1.786(4) 0.03 [45]	122(1)[b] 7 [38]	104.3(2) 2 [80]	99.3(4) 2 [32]
	Ag(I)	2.43(4) 0.08 [4]	1.508(7)[d] 0.007 [2]	1.80(2) 0.02 [2]	127(4) 9 [4]	105.50(6)[b] 0.1 [4]	99.7(1)[b] 0.1 [2]
12	Zn(II)	2.10(1) 0.03 [4]	1.500(4)[d] 0.006 [4]	1.76(1) 0.02 [4]	122(2) 3 [4]	105.3(5) 1 [8]	98.5(8) 1 [4]
	Cd(II)	2.309(9) 0.055 [38]	1.529(3) 0.014 [30]	1.775(2)[b] 0.01 [40]	124(1) 7 [43]	105.0(2) 1 [70]	98.5(3) 1 [30]
	Hg(II)	2.46(8) 0.2 [9]	1.527(7) 0.017 [8]	1.793(7) 0.01 [7]	122(2) 6 [10]	105.2(4) 1 [16]	98.2(5) 1 [8]
13	Al(III)	1.86(1) 0.02 [2]	1.551(3)[d] 0.004 [2]	1.766(3) 0.010 [4]	122(8) 11 [2]	103.2(4) 0.8 [4]	100.3(6) 0.8 [2]
	In(III)	2.18(1) 0.03 [5]	1.534(4) 0.008 [5]	1.774(3) 0.007 [8]	123.8(3)[b] 0.8 [7]	103.7(4) 1 [14]	98.9(6) 1 [7]
	Tl(III)	2.42(2)[e]	1.49(2)[e]	1.74(3)[e]	124(1)[e]	100(1)[e]	97(1)[e]
14	Sn(IV)	2.30(3) 0.16 [24]	1.531(5) 0.021 [25]	1.789(6) 0.03 [24]	126(1) 6 [25]	104.1(3) 2 [43]	99.5(5) 2 [23]
	Pb(II)	2.40(3) 0.09 [9]	1.527(8) 0.02 [7]	1.77(2) 0.03 [5]	128(2) 7 [9]	104.4(4) 1 [18]	98.0(4)[d] 0.8 [8]
15	Bi(III)	2.48(1) 0.04 [11]	1.528(5) 0.007 [3]	1.776(4)[b] 0.009 [6]	126(1) 4 [13]	104.4(4) 0.9 [8]	98.5(7) 1 [4]

[a] Ln: La, Ce, Nd, Eu, Gd, and Er.
[b] Unweighted mean.
[c] Data calculated from C.S.D., for the −70 °C structure [140].
[d] Weighted mean.
[e] One value only.
[g] Dirhodium complexes with a metal–metal bond.
[f] Cyclic sulfoxide.

Table 4
Average dimensions for S-bonded metal sulfoxide complexes

Group	M	M–S	S–O	S–C	M–S–O	M–S–C	O–S–C	C–S–C
6	Cr(0)[a,*]	2.331(1)	1.486(3)	1.811(5)	114.6(1)	117.0(6)	106.5(3)	92.6(2)
7	Tc(III)	2.289(3)[b] 0 [2]	1.476(7)[b] 0.0007 [2]	1.805(7)[b] 0.01 [4]	119.3(4)[b] 0.4 [2]	112(1) 2.0 [4]	106.4(6) 0.9 [4]	98.0(6)[b] 0.7 [2]
	Re(I)	2.349(1)[a]	1.462(4)[a]	1.777(9) 0.009 [2]	118.5(3)[a]	111(2) 2 [2]	107.5(9) 1 [2]	99.7(4)[a]
8	Fe(II)	2.25(5) 0.08 [2]	1.464(7)[c] 0.009 [2]	1.82(2) 0.04 [3]	116(2) 3 [2]	114.0(9) 2 [4]	107(1) 2 [4]	96.4(6)[b] 0.2 [2]
	Ru(II)[d]	2.260(2) 0.024 [175]	1.480(1) 0.013 [167]	1.784(1) 0.016 [306]	117.6(2) 2 [168]	112.8(1) 3 [333]	106.22(7) 1 [336]	99.2(1) 1 [154]
	Ru(II)[e,f]	2.329(5) 0.028 [33]	1.474(3) 0.013 [33]	1.793(4) 0.030 [50]	116.7(4) 2 [33]	111.9(5) 4 [62]	107.2(3) 2 [62]	100.3(7) 4 [31]
	Ru(III)[d]	2.267(7) 0.029 [20]	1.481(3) 0.012 [20]	1.780(2) 0.012 [32]	115.8(7) 3 [19]	113.3(3) 1.8 [32]	106.7(2) 1 [38]	99.3(3) 1 [19]
	Ru(III)[e]	2.343(3) 0.01 [10]	1.472(3) 0.009 [10]	1.779(3) 0.012 [20]	117.1(3) 1 [10]	112.4(3) 1 [20]	107.4(2) 0.9 [20]	99.7(4) 1 [8]
	Os(II)	2.33(1) 0.03 [4]	1.476(7) 0.013 [4]	1.781(7) 0.014 [6]	115(1) 1.5 [2]	114(2) 3.8 [3]	107.0(7) 2 [6]	101(1) 2 [4]
9	Rh(II)	2.45(2) 0.06 [17]	1.478(5) 0.017 [13]	1.782(3) 0.014 [25]	122.3(7) 3 [17]	108.6(3) 2 [28]	107.6(2) 1 [24]	99.6(4) 1 [12]
	Rh(III)[d]	2.267(8) 0.032 [16]	1.467(3) 0.009 [13]	1.776(4) 0.016 [18]	115.2(3) 1 [13]	112.2(3) 1 [24]	107.9(3) 2 [26]	100.7(5) 2 [13]
	Rh(III)[e]	2.323(3) 0.010 [11]	1.464(5) 0.015 [11]	1.771(2)[c] 0.008 [22]	116.1(3) 0.9 [11]	111.9(2) 0.7 [19]	107.9(3) 1 [22]	100.1(2) 0.6 [11]
	Ir(I)	2.18(2) 0.05 [6]	1.475(2)[b] 0.003 [6]	1.804(7) 0.02 [12]	120.5(5) 1 [6]	109(1) 4 [12]	106.6(2) 0.6 [12]	103.1(8) 2 [6]
	Ir(III)	2.27(1) 0.06 [20]	1.473(4) 0.011 [11]	1.766(5) 0.019 [22]	117.0(5) 2 [14]	112.2(7) 3 [27]	107.0(3) 1 [26]	100.0(6) 2 [12]
10	Pd(II)[d]	2.233(5) 0.021 [18]	1.467(4) 0.013 [17]	1.779(4) 0.016 [20]	115.7(7) 2 [12]	109.5(6) 3 [26]	108.8(2)	101.5(6)[c] 0.8 [2]
	Pd(II)[e]	2.296(5) 0.006 [2]	1.476(5)[a]	1.778(7)[b] 0.003 [2]	113(1) 2 [2]	112(1) 2 [4]	108.6(3)[c] 0.7 [4]	
	Pt(I)	2.171(4)[b] 0.008 [5]	1.49(2) 0.03 [2]	1.80(1)[b,g] 0.02 [9]	121.4(4)[b] 0.7 [5]	111(2) 4 [7]	106.3(5)[b] 1 [7]	100.0(8)[b] 1 [3]
	Pt(II)[d]	2.216(2) 0.025 [151]	1.467(1) 0.012 [150]	1.781(1)[c] 0.016 [159]	116.4(2) 2.0 [148]	110.6(3) 2.5 [233]	108.3(1) 1.5 [285]	101.4(2) 2.3 [140]
	Pt(II)[e]	2.275(9) 0.018 [4]	1.474(4)[b] 0.005 [4]	1.792(6)[b] 0.008 [4]	118(1) 2 [4]	110(1) 3 [8]	108.4(8) 1.6 [4]	100.1(4)[b] 0.5 [2]
	Pt(IV)	2.31(2) 0.02 [2]	1.449(6)[a]	1.76(1) 0.01 [2]	112(1) 2 [2]	109.9(8) 1 [2]	*	*

[a] One value only.
[b] Weighted mean.
[c] Unweighted mean.
[d] S-bonded sulfoxides not *trans* to S.
[e] S-bonded sulfoxides *trans* to S.
[f] One S-bonded sulfoxide.
[g] From not accurate data.
[*] Tmso complex.

1.513±0.005 Å (H-bonded sulfoxides), and 1.541±0.007 Å (2:1 protonated sulfoxides). The hypothesis that the difference of 0.021 Å, between free and H-bonded sulfoxides, and that of 0.028 Å, between H-bonded and protonated species $[(\text{sulfoxide–O})_2\text{H}]^+$, are statistically significant was verified by 'two-sided' tests at the 98% significance level [97a].

Tables 3 and 4 list the semi-weighted means for some structural parameters of the O- and S-bonded metal

Table 5
Statistics of bond lengths (Å) and angles (°) in O-bonded metal sulfoxide complexes

	S–O	S–C	M–O–S	C–S–C	O–S–C
Minimum	1.470	1.600	111.3	86.0	97.0
Maximum	1.578	1.960	161.3	122.0	120.2
n	291	413	323	286	586
Median	1.527	1.779	123.6	98.9	104.20
q_l	1.517	1.770	120.6	98.0	103.2
q_u	1.540	1.790	128.6	99.8	105.4
σ	0.018	0.027	8.1	2.5	1.9
$\langle\sigma_i\rangle$	0.006	0.009	0.4	0.6	0.5
Skewness	−0.102	0.693	0.40	4.9	1.5
$\langle x\rangle_u$	1.5275	1.7805	125.66	99.00	104.34
$\sigma(\langle x\rangle_u)$	0.0011	0.0013	0.45	0.15	0.08
$\langle x\rangle_s$	1.5279	1.7804	125.66	98.98	104.33
$\sigma(\langle x\rangle_s)$	0.0012	0.0014	0.45	0.16	0.08
$\langle x\rangle_w$	1.5308	1.7823	124.76	98.88	104.18
$\sigma(\langle x\rangle_w)$	0.0003	0.0003	0.02	0.02	0.01
$C_{0.98}$	±0.0025	±0.0031	±1.05	±0.35	±0.19

Table 7
Observed values of the S–O stretching frequency (ν, cm^{-1}) and bond distance (d, Å) for dmso and metal sulfoxide complexes

Compound	ν	d
dmso (gas, 360 K)	1101[a]	1.485(6)[b]
dmso (liquid, 300 K)	1058[a]	
dmso (liquid, 213 K)	1044[c]	
dmso (CCl_4, 0.1 M solution, 300 K)	1070[a]	
dmso (solid, 93 K)	1037, 1067[a]	1.492(1)[d]
dmso (solid, 213 K)	1043[c]	1.492(1)[d]
dmso (H_2O (x_{dmso}, 0.2–0.5))	1014, 1050[e]	
Sulfoxide–S metal complexes	1080–1154[f]	1.457–1.491[f]
Sulfoxide–O metal complexes	862–997[f]	1.515–1.556[f]

[a] Ref. [108].
[b] Ref. [112].
[c] Ref. [109].
[d] Mean value at room temperature (Table 1).
[e] Ref. [139].
[f] This work (Table 17).

complexes, whose values were used to evaluate the overall mean values reported in Tables 5 and 6.

The $\langle x\rangle_s$ values of the S−O bond distances with their $C_{0.98}$ values are of 1.5279±0.0025 and 1.4738±0.0015 Å, respectively, for O- (Table 5) and S-bonded (Table 6) metal complexes. As in the case of uncoordinated sulfoxides (Tables 1 and 2), the distributions are close to normality and nearly symmetrical, and the semiweighted means are close to the unweighted means. Again, the environmental effects are important. It seems likely that, in this case, they are essentially due to the different electronic effects arising from the different nature of metal atoms and ancillary ligands. The above mean values show that, in agreement with the previous observations [4,5], the S–O bond length is reduced by 0.018 Å upon S-coordination, with respect to free sulfoxides, and increased by 0.036 Å upon O-coordination. Interestingly, the value for O-bonded metal complexes falls between that of H-bonded and that of protonated sulfoxides, $[(sulfoxide–O)_2H]^+$.

The lengthening of the S–O bond distance increases with the increase of the interaction with the oxygen atom, namely from simple H-bonded sulfoxides to O-coordinated metal complexes, up to $[(sulfoxide–O)_2H]^+$ species. It had been also shown that the S–O bond distance is even longer in the 1:1 protonated species, such as $[(dmso–O)H]^+$ (S–O, 1.585(8) Å) and $[(tmso-O)H]^+$ (S–O, 1.589(3) Å) [4]. This trend implies a strengthening of the S–O bond in S-bonded complexes and its weakening in the O-bonded complexes, consistent with the trend of the S–O stretching frequencies (Table 7). This point will be discussed in Section 3.3.

Table 6
Statistics of bond lengths (Å) and angles (°) in S-bonded metal sulfoxide complexes

	S–O	S–C	M–S–O	M–S–C	C–S–C	O–S–C
Minimum	1.398	1.700	109.4	99.8	89.3	99.5
Maximum	1.524	1.911	129.5	120.3	112.1	114.8
n	474	732	477	863	441	922
Median	1.473	1.781	117.0	111.9	100.0	107.1
q_l	1.463	1.773	115.5	110.1	99.0	106.2
q_u	1.482	1.790	118.9	113.7	101.6	108.4
σ	0.014	0.018	2.6	3.0	2.2	1.7
$\langle\sigma_i\rangle$	0.006	0.007	0.3	0.3	0.4	0.4
Skewness	−0.294	1.24	0.40	−0.61	0.45	0.08
$\langle x\rangle_u$	1.4731	1.7836	117.15	111.70	100.35	107.41
$\sigma(\langle x\rangle_u)$	0.0006	0.0007	0.12	0.10	0.11	0.06
$\langle x\rangle_s$	1.4738	1.7837	117.15	111.72	100.33	107.35
$\sigma(\langle x\rangle_s)$	0.0007	0.0008	0.12	0.10	0.11	0.06
$\langle x\rangle_w$	1.4777	1.7829	117.27	112.16	100.54	106.99
$\sigma(\langle x\rangle_w)$	0.0002	0.0002	0.01	0.01	0.01	0.01
$C_{0.98}$	±0.0015	±0.0016	±0.27	±0.24	±0.25	±0.14

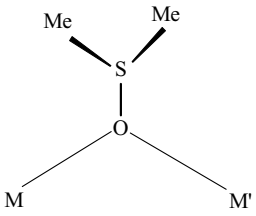

Scheme 1.

2.1.5. Bonding modes

2.1.5.1. Monosulfoxides. The data reported in Section 2.1.3 confirm the previous observations that S-bonding is preferred by the platinum group metal atoms, while the other metals prefer O-bonding [1–4].

In the case of S-coordination, only the η^1–S bonding mode has, so far, been observed while in the case of O-coordination to non-alkali metals, some μ–O metal complexes were found by X-ray analysis in addition to the most common η^1–O bonding mode (Scheme 1).

These include the following cases, for which the mean S–O distance and the relative standard error are reported: $M = M' =$ V(IV), 1.492(5) Å [98]; Rh(II), 1.505(5) Å [7]; Ag(I), 1.509(5) [99]; Cd(II), 1.546(2) Å [100]; Hg(II), 1.51(1) Å [101–103]; Sn(IV), 1.527(1) Å [104]. With the exception of the Cd(II) and Sn(IV) complexes, these bond lengths lie in the shortest part of the range of the S–O bond distances found in η^1–O complexes (Table 5), being shorter than the lower quartile value of 1.517 Å.

The μ–S,O bridging type has been observed in ruthenium or platinum S-bonded sulfoxide complexes interacting with alkali metal ions [4,5], but more recently, a few complexes were reported where sulfoxides act as μ–S,O bridging bidentate ligands connecting two transition metal atoms: $[Ru_2Cl_2(\mu$–dmso–S,O) (μ–Cl) (μ–H) (dmso–S)$_4]$ [105], $[Ru_2Cl_4(CO)_2(\mu$–Cl) (μ–dmso–S,O) (dmso–S)$_3]$ (**1**) [106], $[Ru_3Cl_2(\mu$–mpso–S,O)$_2(\mu$–Cl)$_4$(mpso–S)$_4]$ [54], and [Rh$_2$Cl(cyclooctene) (μ–Cl) (μ–dmso–S,O) (dmso–S)$_2$] [64]. This unusual bonding mode has also been found, in the solid state, in the oligomeric dirhodium(II) tetra(trifluoroacetate) species, $[Rh_2(O_2CCF_3)_4]_m(dmso)_n$, with $m = 7$, $n = 8$ and $m = 3$, $n = 2$ (**2**) [7] (Scheme 2).

From the data reported in Table 8 for the three ruthenium(II) complexes, it appears that in the μ–S,O ligand the S–O distance (1.507(5)–1.532(4) Å) is markedly longer than in the η^1–S ligands (1.442(5)–1.486(6) Å), approaching the mean value of 1.542(4) Å of the η^1–O complexes (Table 3). The same trend is also observed in the Rh(I) complex (1.521(2) Å versus 1.480(2) Å). Too few data are available for a discussion of the Ru–S and Ru–O distances in the μ–S,O complexes, in comparison with the η^1–S/O complexes. However, it seems (Table 8) that on the average the Ru–S bond distances are slightly shorter than in the monodentate η^1–S complexes, while the Ru–O distances (2.122(5)–2.199(4) Å) are slightly longer than the η^1–O mean value of 2.123(7) Å (Table 3).

In the two dirhodium(II) tetra(trifluoroacetate) oligomers the trend of the bond distances is much less clear. In the $m = 7$, $n = 8$ species, the average S–O distance in the μ–S,O ligands (1.49(1) Å) is, as expected, longer than that in the η^1–S Rh(II) complexes (1.478(5) Å, Table 4), but the difference is not significant, and the same value is found in the terminal η^1–O group (Table 8). On the other hand, in the $m = 3$, $n = 2$ complex, the S−O distance in the μ–S,O ligands is as short as 1.465(8) Å, a value that would be more appropriate for an η^1–S species. On the contrary, the Rh−S bond distance (2.449(3) Å) has its normal value (2.45(2), Table 4) and the Rh−O distance of 2.24(1) Å is comparable with that of the η^1–O complexes (2.238(9) Å, Table 3).

2.1.5.2. Disulfoxides. The few X-ray structures reported so far for metal disulfoxide complexes have shown that disulfoxides act as S,S-chelating ligands with palladium, platinum and ruthenium, while they behave as bis-monodentate O-ligands in tin and copper complexes [5]. The only known exception is represented by the [*cis*-PtCl$_2$(PEt$_3$)]$_2$(μ–*meso*–bpse–S,S) complex, in which the disulfoxide acts as an S-bridging ligand, forced by electronic effects [5].

Recent investigations have shown that btse acts as an S,S-chelating ligand with Pd(II), Pt(II), Rh(I), and Ir(I) to form compounds of formula MCl$_2$(btse–S,S) for M = Pd, Pt, and [M(cyclooctadiene) (btse–S,S)](BF$_4$), [M(μ–Cl) (btse–S,S)]$_2$ for M = Rh, Ir [16]. This work by Evans et al. [16] is of particular interest for the potential applications to

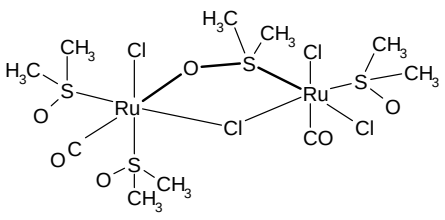

1

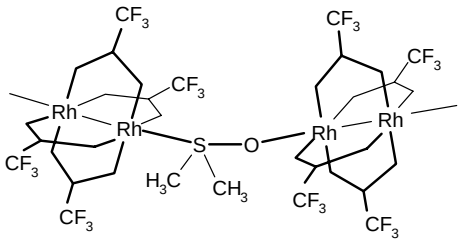

2

Scheme 2.

Table 8
Coordination and S–O bond distances (d, Å) with S–O bond stretching frequencies (ν, cm^{-1}) for transition metal complexes containing μ–S,O sulfoxide ligands

Complex	Bonding mode	d(M–S)	d(S–O) [d(M–O)]	ν(S–O)
$Ru_2Cl_2(\mu$–Cl) (μ–H) (dmso–S)$_4$ (μ–dmso–S,O)[a]	η^1–S	2.223(2)	1.486(4)	1017
		2.232(2)	1.485(4)	
		2.263(2)	1.481(4)	
		2.313(2)[b]	1.442(5)	1093
	μ–S,O	2.188(2) [2.160(4)]	1.532(4)	966
$Ru_2Cl_4(CO)_2$ (μ–Cl) (μ–dmso–S,O) (dmso–S)$_3$[c]	η^1–S	2.282(2)	1.480(5)	1107
		2.291(2)	1.472(6)	
		2.283(2)	1.455(7)	1141
	μ–S,O	2.275(2) [2.122(5)]	1.508(5)	1010
Ru_3Cl_2 (μ–Cl)$_4$ (μ–mpso–S,O)$_2$ (mpso–S)$_4$[d]	η^1–S	2.227(2)	1.486(6)	1088
		2.220(3)	1.466(6)	
		2.192(2)	1.458(6)	
		2.241(2)	1.448(6)	1124
	μ–S,O	2.204(2) [2.191(5)]	1.518(5)	980
		2.214(2) [2.199(4)]	1.507(5)	1004
[Rh_2Cl(cyclooctene) (μ–Cl) (μ–dmso–S,O) (dmso–S)$_2$][e]	η^1–S	2.161(1)	1.479(2)	–[f]
		2.197(1)	1.480(2)	
	μ–S,O	2.158(1) [2.112(2)]	1.521(2)	–[f]
[$Rh_2(O_2CCF_3)_4$]$_7$ (μ–dmso–S,O)$_6$ (dmso–O)$_2$[g]	η^1–O	[2.24(1)]	1.49(1)	1028
	μ–S,O	2.522(5) [2.23(1)]	1.47(1)	1079
		2.451(4)] [2.23(1)]	1.50(1)	
		2.410(4) [2.27(1)]	1.50(1)	
{[$Rh_2(O_2CCF_3)_4$]$_3$ (μ–dmso–S,O)$_2$}$_\infty$[g]	μ–S,O	2.449(3) [2.219(7)]	1.465(8)	1099

[a] Ref. [105].
[b] *trans* to H.
[c] Ref. [106].
[d] Ref. [54].
[e] Ref. [64].
[f] IR data not reported.
[g] Ref. [7].

asymmetric catalysis, reporting the facile synthesis and characterization of enantiomerically pure complexes containing bidentate R_S,R_S–btse ligands (prepared from optically pure R_S–*p*-tolyl-methylsulfoxide). The structural results show that the chelate rings are both sterically and electronically dissymmetric, in spite of their pseudo-C_2-symmetry [16].

On the other hand, as expected, bmse and bpsp act as μ–O,O ligands with Cu(II) [17]. After separation, by fractional crystallizations, of the *meso* (α) and *rac* (β) forms of the two disulfoxides, the following copper complexes were structurally characterized, [Cu(*meso*–bpsp–O,O)$_2$(H_2O)$_2$](ClO_4) (**3**), [Cu(*meso*–bmse–O,O)$_2$](ClO_4)$_2$ (**4**), [Cu(*rac*–bmse–O,O)$_2$](ClO_4)$_2$ (**5**) [17]. The crystal structures of the *meso* complexes **3** and **4** consist of chains in which the copper atoms, aligned on inversion centers, are linked by two disulfoxide–O bridges forming, respectively, 16- and 14-membered puckered rings. The metal atoms achieve an octahedral environment by coordination in *trans* positions to the oxygen atoms of H_2O (**3**) or ClO_4^- (**4**). A different structure is found in the *rac* isomer (**5**), characterized by layers with a 'net' structure, formed by meshes of 28 atoms, including four copper atoms. Again, the octahedral coordination geometry of the metal atoms is provided by *trans* perchlorate anions. Since the copper atoms lie on inversion centers, in each mesh two adjacent bmse ligands have R_SR_S configurations, and the other

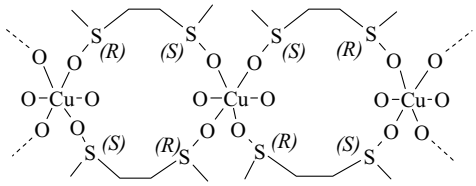

4

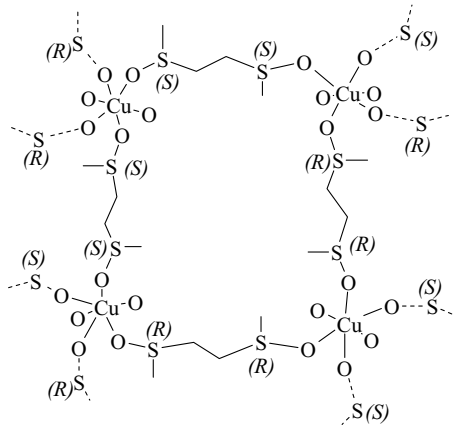

5

Scheme 3.

two have S_SS_S configurations (Scheme 3). A layer structure has also been found in the Cu(II) *rac*-bpsp complex, [Cu(*rac*–bpsp–O,O)$_2$(ClO_4)](ClO_4) [107]. Here, however, the copper atoms exhibit a square pyramidal geometry and the crystals consist of alternate homochiral polycationic layers in which the equatorial CuO_4 groups are displayed according to a 'chess-board' structure [107].

2.2. IR spectroscopy data

The IR spectrum of dmso has been measured in various physical states (Table 7), showing that ν(SO) is of 1101 cm^{-1} in the gas phase, 1070 cm^{-1} in CCl_4 solution, 1058 cm^{-1} in the liquid state, and 1055 cm^{-1} in the solid state [108].

Since the first investigations, the S–O stretching frequencies were used to distinguish O- from S-bonding [1]. In fact, compared to free dmso, ν(SO) increases for S-bonded species (1080–1154 cm^{-1}) and decreases for O-bonded species (862–997 cm^{-1}), paralleling the variation of the S–O bond distances (Table 7).

In the case of μ–dmso–O complexes, the trend of the S–O stretching frequencies and bond distances is not so straightforward. For example, in the vanadium complex (VO)$_2$(2,6-bis(salicylideneaminomethyl)-4-methylphenolato)(CH_3O) (μ–dmso–O), a strong band at 956 cm^{-1} has been observed [98], comparable with the S−O stretching frequency in η^1–O complexes (Table 7). This suggests a weakening of the S–O bond with respect to dmso, but the S–O bond length of 1.492(5) Å corresponds to that of free sulfoxides. In the Rh(II) complex, [$Rh_2(O_2CCF_3)_4$(μ–dmso–O)]$_\infty$, with d(S–O) = 1.505(5) Å, the weak band at 1026 cm^{-1} has been attributed to ν(SO) in the μ–dmso–O group [7]. However, comparison with the above vanadyl value would suggest that the medium intensity band present at 911 cm^{-1} [7] could be attributed to this stretching frequency.

A complicated situation is also found in the μ–S,O complexes, where different steric and electronic effects can play significant roles. In the three Ru(II) complexes reported in Table 8, ν(SO) decreases from 1141–1017 to 1010–966 cm^{-1}, passing from η^1–S to μ–S,O ligands, in agreement with the marked lengthening of the S−O distances (from 1.448(6)–1.486(6) Å to 1.507(5)–1.532(4) Å). Also in this case the ν(SO) values of the bridging ligands are close to the upper range limit of the frequencies found in O-bonded complexes (997–862 cm^{-1}).

A higher stretching frequency is found for the μ–S,O dmso ligand in the case of {[$Rh_2(O_2CCF_3)_4$]$_3$(μ–dmso–S,O)$_2$}$_\infty$ (Table 8), in accord with the very short S–O bond length (1.465 Å) [7]. In fact, the value of 1099 cm^{-1} is well within the range of values (1080–1154 cm^{-1}) found in η^1–S metal complexes. Similarly, in [$Rh_2(O_2CCF_3)_4$]$_7$(dmso–O)$_2$(μ–dmso–S,O)$_6$, the higher stretching frequency (1079 cm^{-1}) is attributed to the μ–S,O ligand, and the lower one (1028 cm^{-1}) to the η^1–O ligand [7]. In this case, however, the S−O bond lengths are comparable within the experimental errors (1.47(1), 1.49(1) Å) (Table 8).

3. Quantum chemical calculations

In the last years, various theoretical investigations have been carried out for studying the solvation and coordination properties of dmso. The relative stability of geometrical and linkage isomers of dmso transition metal complexes has been also investigated. Some results are reviewed here, starting from the gas phase structure of dmso and of some simple dmso adducts, since they provide useful information about the variability of the S–O distance and ion–dmso interactions.

3.1. Structural and thermodynamic features of dmso and its adducts

The structure of dmso has been studied through ab initio MO calculations at the MP2 level using various basis sets [110]. Upon changing the basis set from 6–31G* to 6–31G(2d,p) the S–O bond length decreases from 1.510 to 1.499 Å. By further augmenting the basis set with *f* functions on the sulfur atom, the S–O bond length is further reduced to 1.490 Å, while it increases to 1.503 Å after addition of diffuse *s* and *p* functions on both the S and O atoms [110]. According to this last force field, the calculated structural parameters for dmso are: S–O, 1.503; S–C, 1.800 Å; O–S–C, 106.4; C–S–C, 95.7°, comparable with

Table 9
Optimized geometry parameters from HF/6–31G(d,p) of dmso and its adducts with H_2O, HCl and OH^-, together with the calculated SO stretching frequency (ν)[a]

	dmso	dmso·H_2O	dmso·HCl	dmso·OH^-
S–O (Å)	1.485	1.498	1.655	1.506
S–C (Å)	1.795	1.793	1.798	1.789
O–S–C (°)	106.7	106.5	95.5	108.6
C–S–C (°)	97.8			
ν(SO) (cm^{-1})	1172	1147[b], 1063[c]	1180[b], 1122[c]	-[d]

[a] Ref. [113].
[b] Symmetric stretching mode.
[c] Asymmetric stretching mode.
[d] Not calculated.

the results of G2(MP2)-B3LYP/6–31+G(2df,2p) calculations [111], which provided the following structural parameters: S–O, 1.496; S–C, 1.824 Å; O–S–C, 106.6; C–S–C, 96.6°. All these values show a more or less significant overestimation of the bond distances with respect to the gas phase experimental values, while bond angles are well reproduced: S–O, 1.485; S–C, 1.799 Å; O–S–C, 106.0; C–S–C, 96.6° [112].

When the molecular structure of dmso was calculated by ab initio HF/6–31G** methods, an S–O bond length of 1.485 Å was found [113]. These structural calculations were also extended to the dmso adducts with H_2O (**6**), HCl (**7**), OH^- (**8**) (Table 9), and the S–O bond length was found to increase from dmso to the H_2O (**6**, 1.498 Å), OH^- (**8**, 1.506 Å), and HCl (**7**, 1.655 Å) adducts [113] (Scheme 4).

For a comparison, Table 10 reports some dmso parameters calculated with different semi-empirical (AM1 and PM3) and ab initio methods with different basis sets [114].

In order to gain insight into the dmso solvation properties, thermodynamic parameters were measured for the gas phase equilibria

$$X^-(\text{dmso})_{n-1} + \text{dmso} = X^-(\text{dmso})_n$$

with X = Cl (n = 1–5), and Br, I (n = 1–3) [115]. Comparison with the values obtained for the $K^+(\text{dmso})_n$ system shows that the isoelectronic potassium cation binds to dmso much more strongly than Cl^-. MO calculations, at the 4-31G level, for these systems, and improved electrostatic calculations, show that this behavior is due to electrostatic interactions arising from the strongly dipolar nature of the $S^{\delta+}O^{\delta-}$ group [115]. The following scheme depicts the calculated structures of dmso (**9**), K^+(dmso) (**10**), and Cl^-(dmso) (**11**), with the atomic Mulliken charges (q) and ion interaction distances (Scheme 5). In agreement with the experiment ($\Delta H(K^+) = -144.3$, $\Delta H(Cl^-) = -77.8\,\text{kJ mol}^{-1}$), the calculated binding energies (BE) are 165.7 and 87.9 kJ mol^{-1} for the K^+ and Cl^- species, respectively [115]. Electrostatic calculations, including ion–dipole, ion-induced dipole, ion–molecule dispersion attraction and ion–molecule repulsive interactions, give $E(K^+) = -120.5$ and $E(Cl^-) = -87.9\,\text{kJ mol}^{-1}$. These data show that the bonding is essentially electrostatic, with a dominance of the ion–dipole term, as a consequence of the closer approach of the K^+ ion [115].

3.2. Dmso protonation

The study of the protonation of sulfoxides is of particular relevance for the understanding of their interactions with acids, superacids, and electrophiles. It also throws some light upon the nature of the sulfoxide interaction with metal ions.

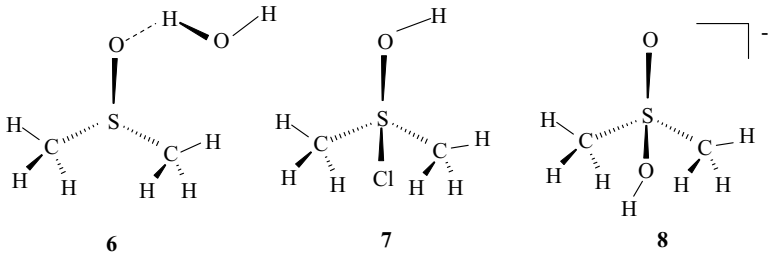

6 **7** **8**

Scheme 4.

Table 10
Molecular geometry of dmso and S, O atomic charges (q, e), calculated with different quantum chemical methods and basis sets

	AM1	PM3	RHF/6–31(d,p)	RHF/6–311++(3df,spd)	RMP2/6–31(d,p)
S–O (Å)	1.491	1.557	1.4854	1.486	1.511
S–C (Å)	1.739	1.818	1.7951	1.797	1.808
O–S–C (°)	105.67	104.61	106.69	106.35	107.42
C–S–C (°)	99.69	99.24	97.82	98.32	95.60
q(O)	−0.7785	−0.6946	−0.7856	−0.5558	−0.7894
q(S)	+1.3939	+0.9428	+0.9443	+0.7433	+0.9449

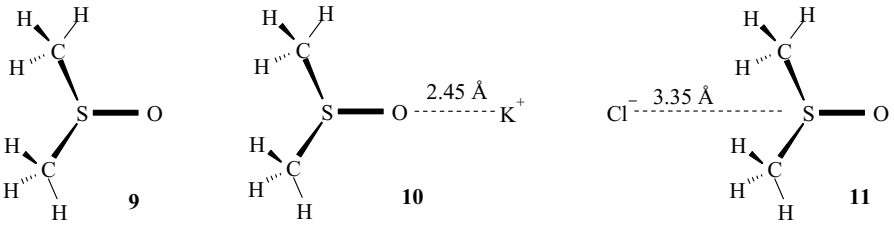

Scheme 5.

MINDO/3 calculations were carried out to investigate the most stable cations formed by protonation of dmso, together with the energetics of the protonation reactions [116] (Scheme 6).

It is quite evident that O-protonation to give **12** is the most favorable process. In fact, even if the calculated heats of reaction cannot be expected to agree with the experimental values, because proton solvation has not been taken into account, the energy difference between the O- and S-protonated species (**13**–**12**, 293.3 kJ mol^{-1}) should not be markedly affected [116]. Calculations also showed a decrease of the atomic negative charge on oxygen, from −0.617 in dmso to −0.461 in the O-protonated cation (**12**), while the positive charge on S does not change significantly from dmso (0.853) to $[(dmso–O)H]^+$ (0.865). On the other hand, with S-protonation (**13**) the charge on sulfur increases to +1.168, whereas it remains approximately the same on oxygen (−0.486) [116].

Diprotonation has been also investigated, indicating again that O-protonation is largely favored yielding the oxonium species **15**, rather than the S-protonated dication **16**, in agreement with the ^{1}H NMR spectrum in HSO_3F–SbF_5 solution [116].

Dmso protonation in the gas phase was also studied by ab initio methods [117], which again indicated preferential protonation on oxygen in dmso. However, at the MP2/6–31G(d,p) level, the proton affinity was overestimated by 64 kJ mol^{-1}, which is comparable to the energy difference between the isomers [117].

Accurate heats of formation (ΔH_f) and proton affinities (PA) for six dmso valence-bond isomers were obtained from G2(MP2) calculations based on B3LYP/6–31+G(dp) optimized geometries [111]. For the lowest calculated energy isomer ($(CH_3)_2S{=}O$, with C_s symmetry), $\Delta H_f(298\,K) = -152.6$ and PA = 885 kJ mol^{-1} were found, in good agreement with the experimental values of $\Delta H_f(298\,K) =$

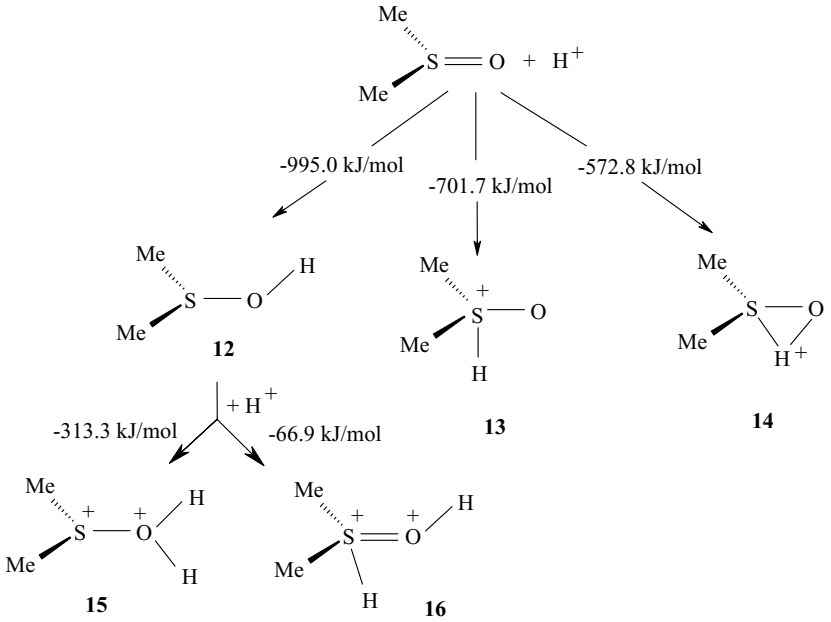

Scheme 6.

−151.3(8), and PA = 882 kJ mol^{-1} [111]. Calculations have also shown that the O-protonated dmso is separated from the other isomers by large potential energy barriers [111].

In recent work, the energies, electronic structures, and thermodynamics of protonated and methylated dmso cations and dications were calculated using density functional theory (DFT) using a B3LYP/6–311+G** basis set [118]. The O-protonated structure (**12**) was found to be 154.8 kJ mol^{-1} more stable than the S–protonated isomer (**13**) [118]. The calculated S–O and S–C bond distances are, respectively: 1.514 and 1.836 Å in dmso, 1.641 and 1.806 Å in $[(dmso–O)H]^+$, and 1.817 and 1.798 Å in $[(dmso–O)H_2]^{2+}$ (**15**), showing a remarkable increase of the S–O bond distance and a decrease of the S–C distances [118]. This trend is in perfect agreement with the results of a principal component analysis (PCA) of the X-ray structural data, which indicated that by increasing the degree of protonation on oxygen, the first principal component, describing 54.9% of the overall variance, for the S–O and S–C bond distances have opposite signs, so that if the former increases, the others decrease [4].

Structural parameters and relative molecular energies of dmso and its protonated species have recently been calculated by DFT methods using BP and VWN functionals, including two 3d and one 4f polarization functions in the sulfur basis set [128]. The best agreement between experimental and calculated structural parameters was obtained in the case of the VWN functional (Table 11). However, both functionals indicate that $[(dmso–O)H]^+$ has a molecular energy 93 kJ mol^{-1} lower than $[(dmso–S)H]^+$, and give similar trends for bond lengths and angles. The VWN results show again that upon O protonation of dmso there is a marked lengthening of the S–O distance (0.113 Å) and a shortening (0.040 Å) of the S–C distances, accompanied by a narrowing (6.2°) of the O–S–C angles, and a widening (5.9°) of the C–S–C angle [128]. This trend is in good agreement with the observed variations of +0.100 Å (S–O), −0.017 Å (S–C), −4.7° (O–S–C), and +4.1° (C–S–C), obtained from the experimental data in Table 11, as well as with the previous PCA results [4].

Table 12
Ranges of observed[a] and calculated[b] vibrational frequencies (cm^{-1}) with assignments for dmso

ν (observed)	ν (calculated)	Assignment
2998–2917	3242–3113	CH_3 stretching
1435–1303	1527–1355	CH_3 bending
1070	1102	SO stretching
1008	1057	CH_3 rocking
945	982	CH_3 rocking, S–O stretching
883–918	927–960	CH_3 rocking
683	723	SC stretching, CH_3 rocking
661	697	SC stretching
329–378	318–377	OSC bending, CH_3 rocking
305	296	CSC bending, OSC bending

[a] Dilute solution in CCl_4 or CS_2 [108].
[b] Ref. [110].

3.3. IR spectra

3.3.1. Dmso and its adducts

Vibrational frequencies, IR intensities, and assignments of the normal modes of dmso were calculated from the equilibrium geometry, obtained by ab initio calculations at the MP2 level with the 6–31G(2d,p) basis set, including *f* functions on the sulfur atom [110]. The calculated and observed vibrational bands for dmso are summarized in Table 12. The calculated vibrational frequencies are close to those of Jitariu et al. [113] after removal of the scale constant (0.89) introduced by these authors for a comparison with the experimental data.

Vibrational frequencies for the dmso adducts with H_2O (**6**) and HCl (**7**) were also calculated (Table 13), from the optimized geometries obtained by ab initio HF/6–31G** calculations [113]. Calculations show that ν(SO) decreases passing from pure dmso (1172 cm^{-1}) to its water adduct **6** (symmetric stretching 1147, asymmetric 1063 cm^{-1}), in agreement with the experimentally observed decrease from 1102 to 1044 cm^{-1} [119]. This is also in agreement with the trend of the calculated S–O bond lengths, 1.485 Å in dmso and 1.498 Å in **6** [113]. In **7**, the S–O distance is calculated to be as long as 1.655 Å, but the calculated symmetric SO

Table 11
Optimized bond distances (Å) and angles (°), atomic Mulliken charges (*q*, e), and scaled total energies *E* (kJ mol^{-1}), for free and protonated dmso, together with experimental parameters

	dmso[a]	$[(dmso–O)H]^+$[a]	$[(dmso–S)H]^+$[a]	dmso[b]	$[(dmso–O)H]^+$[c]
S–O	1.489	1.602	1.432	1.485(6)	1.585(8)
S–C	1.794	1.754	1.736	1.799(5)	1.782(3)
O–S–C	106.8	100.6	115.2	106.8(2)	102.1(5)
C–S–C	94.9	100.8	107.4	96.57(3)	100.7(6)
q(O)	−0.61	−0.53	−0.50		
q(S)	+0.58	+0.82	+0.93		
E	0	−865	−772		

[a] Calculated by the VWN functional.
[b] Observed in gas phase [112].
[c] Observed in $[(dmso–O)H][TeCl_6]\cdot 3dmso$ [29].

Table 13
Calculated vibrational frequencies (cm^{-1}) dor dmso and its adducts with H_2O and HCl[a]

	dmso	dmso·H_2O	dmso·HCl
		3299	4151
CH_3 stretch	3309–3197	3206, 3201	3385–3233
HOH stretch		1802	
CH_3 bend	1607–1481	1593–1153	1602, 1587
			1585
SCH bend			1567
HCH bend			1507, 1482
S–OH deformation			1294
SO stretch	1172	1147, 1063	1180
			1122
SCH rock	1140–993	1055, 1006	1097, 1054
SC stretch	793, 749	800, 752	826, 806
O–H out of plane		681	
SOH deformation			727
CH_3, SOH bend			388
S–OH bend			385
OSC bend	399, 342	402	
O···H stretch		371, 352	
CSC bend	312	315	312
S–OH out of plane			245
ClSO bend			213
S–Cl stretch			202
ClC bend			176
CH_3 tors	253, 206	262, 215	122, 66
OH stretch		171	
HOH rock		161	
O···H–O twist		94	
		34	

[a] Ref. [113].

stretching frequency (1180 cm^{-1}) is comparable with that of dmso (1172 cm^{-1}).

In other studies, the vibrational spectra for dmso [120], and for the $[(dmso–O)H]^+$ cation [121], were calculated, after full geometry optimization, by the ab initio SCF method using a 3–21G(1d) basis set. Ranges of observed and calculated vibrational frequencies for $[(dmso–O)H]^+$ are listed in Table 14. The results are in good agreement with those of Jitariu et al. [113]. As expected, the marked decrease of ν(SO) from dmso (1178 cm^{-1}) to its O-protonated form (933 cm^{-1}) is accompanied by a significant increase of the calculated S−O bond distance, from 1.490 Å in dmso to 1.599 Å in $[(dmso–O)H]^+$ [121].

Table 14
Ranges of observed and calculated vibrational frequencies (cm^{-1}) with assignments for $[(dmso–O)H]^+$

ν (observed)[a]	ν (calculated)[b]	Assignment[b]
3600[c]	3782	ν(OH)
3000–2900	3213–3318	ν(CH)
1470–1350	1545–1624	$\delta(CH_3)$
	1258	$\delta(HOS+CH_3)$
1025–980	1196–1073	$\delta(CH_3+SCH)$
870	933	ν(SO)
730–680	779–710	ν(SC)
	386	$\delta(HOS+SCH+CH_3)$
	359–303	δ(CSO+CSC)
	229	δ(HOS+CSC)

[a] Ref. [141].
[b] Ref. [121].
[c] Ref. [142].

3.3.2. Metal dmso complexes

Ab initio SCF calculations with a 3-21G(1d) basis, including the SBK [122] valence basis set for the platinum atom, were performed to calculate some structural and spectroscopic characteristics of the Pt(II) linkage isomers, $[PtCl_3(dmso–O)]^-$ and $[PtCl_3(dmso–S)]^-$, and of the Pt(IV) complex, $[PtCl_5(dmso–S)]^-$ (Table 15) [123]. As for dmso, the calculated IR spectrum of $[PtCl_3(dmso–S)]^-$ presents two groups of bands at about 3300 and 1500–1600 cm^{-1} (vibrations of the CH_3 groups), two other groups at 1000–1100 and 700–800 cm^{-1} (CH_3 and S–C bond vibrations), and an

Table 15
Calculated S–O stretching frequency (ν, cm^{-1}), bond distances (d, Å), bond orders (n), and effective atomic charges (q, e) for Pt(II) and Pt(IV) dmso complexes[a]

	$[Pt(II)Cl_3(dmso–O)]^-$	$[Pt(II)Cl_3(dmso–S)]^-$	$[Pt(IV)Cl_5(dmso–S)]^-$
ν(S–O)	1022	1220	1241
d(S–O)	1.526	1.479	1.471
n(S–O)	1.22	1.55	1.57
q(S)	1.00	1.01	1.08
q(O)	−0.61	−0.61	−0.58
q(Me)	−0.05	−0.08	−0.05
q(dmso)	0.29	0.24	0.40
d(Pt–O/S)	2.101	2.341	2.432
d(Pt–Cl_{trans})	2.351	3.353	2.320
d(Pt–Cl_{cis})	2.410	2.393	2.365[b]
n(Pt–Cl_{trans})	0.70	0.66	0.73
n(Pt–Cl_{cis})	0.58	0.63	0.73[b]
q(Cl_{trans})	−0.55	−0.55	−0.36
q(Cl_{cis})	−0.63	−0.58	−0.41[b]

[a] Ref. [123].
[b] Average value.

Table 16
Calculated values of S–O stretching frequency (ν, cm^{-1}), bond distance (d, Å), bond index (n), and effective atomic charges (q, e) for dmso, *trans*-$[RuCl_4(CO)\ (dmso–O)]^-$ and $[(dmso–O)H]^+$

	dmso[a]	*trans*-$[RuCl_4(CO)\ (dmso–O)]^-$[b]	$[(dmso–O)H]^+$[c]
ν(S–O)	1178	1061	933
d (S–O)	1.490	1.521	1.599
n(S–O)	1.56	1.22	0.99
q(S)	1.00	1.02	1.08
q(O)	−0.68	−0.65	−0.68
q(Me)	−0.16	−0.06	0.06
q(dmso)	0.00	0.25	0.52

[a] Ref. [123].
[b] Ref. [125].
[c] Ref. [121].

intense band at 1220 cm^{-1} due to the S–O vibration [120]. This last band is shifted to 1022 cm^{-1} in the hypothetical dmso–O isomer, with a reduction of 156 cm^{-1} with respect to dmso, testifying to the weakening of the S–O bond upon O-coordination [121]. Accordingly, the calculated S–O bond distance is lengthened, with respect to dmso, by 0.036 Å. The Pt–S stretching frequencies in the $[PtCl_3(dmso–S)]^-$ spectrum appear as components of a number of bands below 230 cm^{-1} with extremely low intensities [120]. Intense bands in the range 320–330 cm^{-1} are calculated for the Pt–Cl vibrations for both complexes [120].

In $[Pt(IV)Cl_5(dmso–S)]^-$, ν(SO) increases with respect to $[Pt(II)Cl_3(dmso–S)]^-$, from 1220 to 1241 cm^{-1}, in correspondence with the calculated decrease of the S–O bond length from 1.479 to 1.471 Å (Table 15) [123]. These trends are in agreement with those observed for the ν(SO) stretching frequencies and the S–O bond lengths in some Pt(IV) and Pt(II) dmso–S complexes [124].

Similar ab initio SCF calculations were reported for the Ru(III) complex, *trans*-$[Ru(dmso–O)\ (CO)Cl_4]^-$ [125]. Some relevant calculated parameters for dmso, $[(dmso–O)H]^+$ [121], and *trans*-$[Ru(dmso–O)\ (CO)Cl_4]^-$ are reported together in Table 16, for comparison. Once more, it is shown that in O-bonded species the S–O stretching frequency decreases with respect to free dmso, while the S–O bond distance increases.

In order to get an overall view of the relationship betwen S–O stretching frequencies and bond lengths, Table 17 reports the values observed in a series of η^1–S- and O-bonded metal sulfoxide complexes, together with those for free dmso. The plot of these data, together with that of some calculated values (Table 18), confirms the general observation that ν(SO) decreases with the increase of the S–O bond distance (Fig. 1). The values for the S- and O-bonded complexes are neatly separated, above and below those for free dmso, confirming the hypothesis of a weakening of the S–O bond in the O-bonded complexes. The two curves in Fig. 1 represent the best-fit lines for the calculated and observed sets of data, given by second order polynomials.

Table 17
Observed values of the S–O stretching frequency (ν, cm^{-1}) and bond distance (d, Å), in dmso (bold characters) and η^1–S- and O-bonded metal sulfoxide complexes

Complex	d	ν
cis-PtCl(dmso–S) $(C_{16}H_{29}N_2O_3S)$[a]	1.457(4)	1154
cis-$PtCl_2$(mpso–S)$_2$[b]	1.463(1)	1150
cis-$PtBr_2$(dmso–S) (MeCN)[c]	1.468(20)	1150
cis-Pt(dmso–S) $(PhCH_2CN)Cl_2$[d]	1.457(4)	1149
cis-$PtCl_2$(dmso–S) (MeCN)[e]	1.470(7)	1148
cis-$PtCl_2$(dmso–S) (C_2H_4)[d]	1.469(9)	1148
cis-$PtCl_2$(dmso–S) (MeCN)[c]	1.469(5)	1147
$[PtCl_3(dpso–S)]^-$[b]	1.469(8)	1145
$[PtCl_3(dmso–S)]^-$[f]	1.46(2)	1142
[*cis*-PtCl(dmso–S) $(\mu–C_2H_4NO)]_2$[e]	1.461(1)	1141
[*trans*-Pt(pyridine)$_2$Cl(dmso–S)]$^+$[g]	1.46(1)	1140
cis-$PtCl_2$(dpso–S)$_2$[h]	1.462(6)	1130
cis-Pt(dmso–S)$_2$(cbdc)[i]	1.468(8)	1127
$[cis\text{-}Pt(NH_3)_2Cl(dmso–S)]^+$[j]	1.46(1)	1122
[PdCl(ethylenediamine) (dmso–S]$^+$[k]	1.471(2)	1130
trans-$PdCl_2$(dmso–S)$_2$[l]	1.476(5)	1116
[Ir(μ^2–Cl) (btse–S)]$_2$[m]	1.475(3)	1122
[Ir(cod) (btse–S)]$^+$[m]	1.475(2)	1122
[*trans*-$IrCl_4(dmso–S)_2]^-$[n]	1.469(1)	1115
$[Rh(O_2CEt)_2(dmso–S)]_2$[o]	1.48(2)	1095
$[Rh(O_2CPh)_2(dmso–S)]_2$[o]	1.477(7)	1094
$[Rh(O_2Cme)_2(dmso–S)]_2$[o]	1.477(5)	1086
trans-$OsCl_2$(dmso–S)$_4$[p]	1.486	1081
mer-$RuCl_3$(dpso) (dpso–S)[q]	1.463(7)	1128
mer,*trans*-$RuCl_3$(dmso–S)$_2$(dmso)[r]	1.479(7)	1127
[*trans*-$RuCl_4(dmso–S)_2]^-$[r]	1.467(8)	1115
mer-$RuCl_3$(dmso–S) (tmem)[s]	1.476(2)	1115
$[fac\text{-}RuCl_3(dmso–S)_3]^-$[t]	1.482(4)	1102
$[fac\text{-}Ru(dmso)_3(dmso–S)_3]^{2+}$[u]	1.481(7)	1100
$[fac\text{-}RuCl_3(dmso–S)_3]^-$[v]	1.49(1)	1100
$[mer\text{-}RuCl_3(dmso–S)_3]^-$[t]	1.483(4)	1098
cis,*fac*-$RuCl_2$(dmso–S)$_3$$(NH_3)$[w]	1.488(3)	1095
[*trans*-$RuCl_4$(dmso–S) $(NH_3)]^-$[x]	1.479(3)	1088
mer,*cis*-$RuCl_3$(dmso–S) (dmso) (NH_3)[x]	1.479(2)	1088
mer-$RuCl_3(N_2H_5)$ (dmso–S)$_2$[p]	1.489(8)	1084
$[mer\text{-}RuCl_3(dmso–S)_3]^-$[t]	1.488(3)	1083
mer-$RuCl_3$(dmso–S) (MeOH) (acv)[y]	1.486(5)	1082
mer-$RuCl_3$(dmso–S) (H_2O) (acv)[y]	1.479(1)	1081
trans-$RuCl_2$(dmso–S)$_4$[z]	1.491(5)	1080
trans,*cis*-$RuCl_2(NH_3)_2$(dmso–S)$_2$[w]	1.492(2)	1064
	1.508(3)	1043
dmso	**1.492(1)**[aa]	**1043**[ab]
[*trans*-$SnPh_2(NO_3)$ (dmso–O)$_3$]$^+$[ac]	1.547(6)	940
$(HgCl_2$(dpso–O)[ad]	1.51(1)	1008
$(HgCl_2)_3$(dmso–O)$_2$[ae]	1.54(1)	994
[HgMe(dmso–O)]$^+$[af]	1.556(8)	935
Cu_4Cl_6O(dmso–O)$_4$[ag]	1.53(2)	956
$Pd(NO_2)$ (pyi) (dmso–O)[ah]	1.526(2)	997
[PdCl(bipyridyl) (dmso–O)]$^+$[ak]	1.538(3)	925
[*trans*-$OsCl_4$(NO) (dmso–O)]$^-$[ai]	1.569(6)	922
[*trans*-$RuCl_4$(CO) (dmso–O)]$^-$[aj]	1.514(3)	957
fac-Ru(dmso)$_3$(dmso–O)$_3$[u]	1.54(1)	935
cis,*fac*-$RuCl_2$(dmso)$_3$(dmso–O)[al]	1.537(3)	927
$[RuBr_3(NO)$ (dmso–O)]$_2$[am]	1.541(7)	920
mer-$RuCl_3$(dpso) (dpso–O)$_2$[q]	1.53(2)	919
mer,*trans*-$RuCl_3$(dmso)$_2$(dmso–O)[r]	1.545(4)	912
mer,*cis*-$RuCl_3$(dmso) (dmso–O) (NH_3)[x]	1.547(2)	907
mer-$RuCl_3$(CO) (tmso-O)$_2$[an]	1.557(2)	921
	1.575(2)	862

Table 17 (*Continued*)

Complex	*d*	*ν*
trans,*cis*,*cis*-$MoBr_2(NO)_2$(dmso–O)$_2$[ao]	1.521(3)	938
$[(dmso–O)H]^+$[ap]	1.585(8)	870[aq]

[a] Ref. [71].
[b] Ref. [143].
[c] Ref. [144].
[d] Ref. [145].
[e] Ref. [146].
[f] Ref. [70].
[g] Ref. [72].
[h] Ref. [147].
[i] Ref. [148].
[j] Ref. [149].
[k] Ref. [150].
[l] Ref. [151].
[m] Ref. [152].
[n] Ref. [153].
[o] Ref. [154].
[p] Ref. [38].
[q] Ref. [129].
[r] Ref. [155].
[s] Ref. [56].
[t] Ref. [136].
[u] Ref. [156].
[v] Ref. [157].
[w] Ref. [158].
[x] Ref. [159].
[y] Ref. [57].
[z] Ref. [160].
[aa] Average value (Table 1).
[ab] Solid state value [109].
[ac] Ref. [161].
[ad] Ref. [162].
[ae] Ref. [163].
[af] Ref. [164].
[ag] Ref. [165].
[ah] Ref. [166].
[ai] Ref. [167].
[aj] Ref. [168].
[ak] Ref. [130].
[al] Ref. [30].
[am] Ref. [168].
[an] Ref. [32].
[ao] Ref. [169].
[ap] Ref. [29].
[aq] Ref. [170].

Table 18
Calculated values for the S–O stretching frequency (ν, cm^{-1}) and bond distance (*d*, Å), in dmso and η^1–S- and η^1–O-bonded metal sulfoxide complexes

Complex	*d*	*ν*
$[PtCl_5(dmso–S)]^-$[a]	1.471	1241
$[PtCl_3(dmso–S)]^-$[a]	1.479	1220
dmso[a]	1.490	1178
[*trans*-$RuCl_4$(dmso–O) (CO)]$^-$[b]	1.521	1061
$[PtCl_3(dmso–O)]^-$[c]	1.526	1022
$[(dmso–O)H]^+$[c]	1.599	933

[a] Ref. [123].
[b] Ref. [125].
[c] Ref. [121].

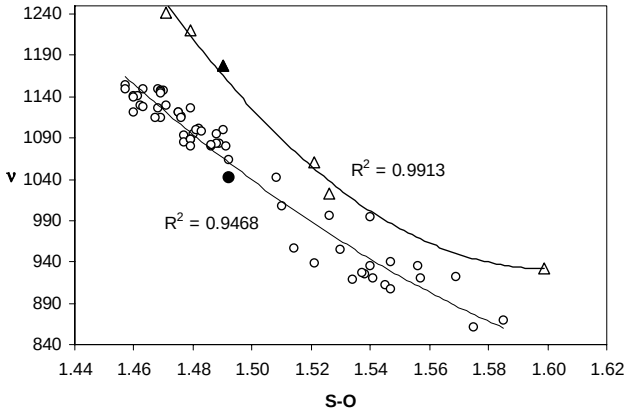

Fig. 1. Plot of observed (circles) and calculated (triangles) S–O bond lengths (Å) and stretching frequencies (ν, cm^{-1}) (Table 17) with interpolation curves and correlation coefficients. The full circle and triangle correspond to 'free' dmso data.

3.4. Metal–sulfoxide bonding

The trends of the bond distances and stretching frequencies in platinum and ruthenium complexes were rationalized considering the electron density redistribution passing from dmso to coordinated dmso [119,121–123], on the basis of the atomic electronegativity equalization concept [127]. The sulfur atom in free dmso has a large positive charge (Table 16) and, as a consequence, a high electronegativity. The metal coordination of the sulfur atom raises its positive charge and hence its electronegativity. Consequently, the methyl groups will, to a considerable extent, compensate for this electron density transfer, in order to reduce the electronegativity of the sulfur atom. Similarly, there is additional transfer of electron density from O to S ($O\pi \rightarrow S\pi$) which leads to an increase of the double bond character of the S–O bond and, therefore, to a decrease of its bond length.

In the case of O-coordination, the electron density on the oxygen atom is reduced with respect to free dmso, and, therefore, the O atom electronegativity is raised. Due to the equalization of the atom electronegativities, this is compensated by electron transfer from the sulfur atom and the methyl groups, which significantly increases the positive charge on the S atom, whereas the negative charge of the O atom changes only slightly in comparison with free dmso. Furthermore, because of the increased O electronegativity, the π-electron transfer to S decreases, reducing the S–O bond order. As a result, the S–O bond is weakened and its bond length is increased.

This scheme is illustrated in Fig. 2a for the two platinum linkage isomers, $[Pt(II)Cl_3(dmso–O)]^-$ and $[Pt(II)Cl_3(dmso–S)]^-$ with the indication of the net electron charge transfers (Table 15). As expected, the calculated S–O bond distance is 1.526 Å in the O-bonded isomer and 1.479 Å in the S-bonded isomer, values that are, respectively, longer and shorter than that found in free dmso.

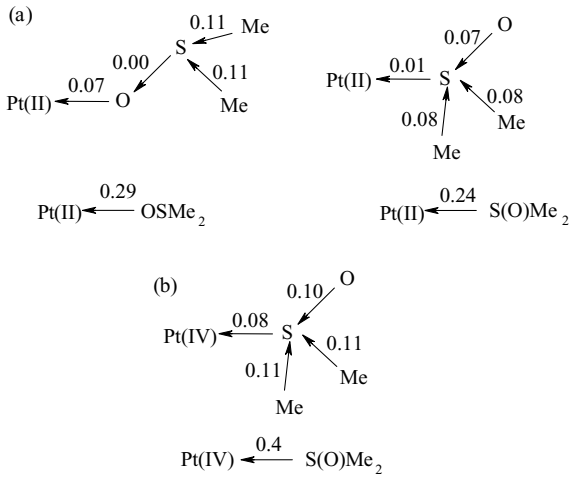

Fig. 2. Sketch of calculated charge transfers in platinum sulfoxide complexes.

A significantly greater charge transfer from dmso–S to platinum is found in the case of the $[Pt(IV)Cl_5(dmso–S)]^-$ complex, as expected from the higher electronegativity of the Pt(IV) metal atom (Fig. 2b). In fact, the S–O bond distance is further reduced to 1.471 Å (Table 15).

According to these calculations [123], the Pt–Cl bonds are shorter and exhibit higher bond orders in $[Pt(IV)Cl_5(dmso–S)]^-$ than in $[Pt(II)Cl_3(dmso–S)]^-$ (Table 15). This explains the longer Pt(IV)−S calculated bond length, in agreement with the crystallographically observed trend (Pt(IV)−S, 2.301 Å; Pt(II)−S, 2.292 Å [4]). In spite of the greater σ donor power of dmso in the Pt(IV) complex, the Pt–S bond is weakened because of charge dissipation over the Pt–Cl bonds, because of the high charge density transfer to the σ-bonding metal orbital from the *trans* chloride ligands.

On the basis of the same scheme, the S–O bond length of 1.506 Å calculated for the $[dmso·OH]^-$ adduct (**8**), could be qualitatively rationalized considering the low electronegativity of the OH^- ion, and hence the reduction of the positive charge on the sulfur atom, which prevents the shortening of the S–O distance, found in the case of S-coordination to positive metal ions. A similar effect could occurr in the dmso·HCl adduct (**7**), in which the lengthening of the S–O bond distance upon protonation of the O sulfinyl group, is not contrasted by the S-coordination of the Cl^- ligand. In fact, the calculated S–O bond distance is of 1.655 Å.

As is well known, [1] S-bonding is favored in the case of 'soft' metal atoms where the sulfoxides act as moderate π-acceptor ligands, so that the metal to sulfur bond is strengthened when S is *trans* to a σ donor ligand and weakened when *trans* to a π accepting ligand.

In order to further investigate this last aspect, the nature of the lowest virtual orbitals of dmso has been examined by DFT methods using the BP functional [128]. Calculations show that, of the almost degenerate empty orbitals 8a″, 15a′ and 16a′, the first is delocalized over π*(S–O) and π*(S–C) orbitals, with a prevalence of the S–O antibonding character. This 8a″ orbital should play the major role in the back-donation from the metal to the coordinated dmso–S ligand. The other two orbitals, 15a′ and 16a′, have mainly S 3d and σ*(C–H) character, respectively [128].

In the same work, the effect of π back-bonding on the Ru(II)–S and S–O bond lengths has been examined on the 'model' molecules $[cis,fac\text{-}Ru(NH_3)_2H_3(dmso–S)]^-$ (**17**) and $[Ru(CO)_5(dmso–S)]^{2+}$ (**18**), in which, respectively, the role of σ-donor and π-acceptor ligands is emphasized [128]. The calculated Ru–S and S–O bond lengths are 2.187 and 1.553 Å, respectively, in **17**, and 2.513 and 1.463 Å in **18**. This trend supports the assumption [4] that the presence of σ-donor ligands, such as NH_3 and H^-, strengthens the Ru–S bond by π back-bonding, with consequent weakening of the S–O bond. On the contrary, π-accepting ligands such as CO weaken the Ru–S bond, and strengthen the S–O bond. Interestingly, the calculated S–C bond distances are 1.875 Å in **17** and 1.810 Å in **18**, in agreement with the partial S–C antibonding character of the 8a″ dmso virtual orbital. In fact, the calculated (BP functional) S–O and S–C bond distances for dmso are 1.507 and 1.834 Å, respectively [128]. In a limiting case, such as that of **18**, the Ru–S bond distance is so long to actually correspond to a non-bonding distance, so that the dmso–S isomer is expected to be unstable in favor of the dmso–O isomer.

The preference for S- or O-bonding of dmso in Ru(II) complexes has been investigated by calculation of the binding energy of the dmso ligand in S- (BE^S) and O- (BE^O) linkage isomers of $cis,fac\text{-}RuCl_2(CO)_3(dmso)$ and $[Ru(NH_3)_5(dmso)]^{2+}$. Calculations were performed by the BP DFT method [128]. As shown in Table 19, O-bonding appears to be preferred in the carbonyl complex ($BE^O > BE^S$), while S-bonding is preferred in the ammonia complex ($BE^S > BE^O$), in agreement with the observation that only the $cis,fac\text{-}RuCl_2(CO)_3(dmso–O)$ and $[Ru(NH_3)_5(dmso–S)]^{2+}$ complexes were isolated [4].

The BE^S values also provided some information about the relative stability of the geometrical isomers of $RuCl_2(dmso)_4$. From Table 19, we can observe that passing from $trans\text{-}RuCl_2(dmso–S)_4$ to $cis,fac\text{-}RuCl_2(dmso–S)_3(dmso–O)$ there is a significant increase of the Ru–dmso–S binding

Table 19
Binding energies ($kJ\,mol^{-1}$) for dmso–S and dmso–O ligands in Ru(II) complexes

Complex	dmso–S	dmso–O
$cis,fac\text{-}RuCl_2(CO)_3(dmso)$	110	132
$[Ru(NH_3)_5(dmso)]^{2+}$	225	200
$cis,fac\text{-}RuCl_2(dmso–S)_3(dmso–O)$	172[a], 208[b]	
$trans,mer\text{-}RuCl_2(dmso–S)_3(dmso–O)$	140[c], 230[b]	
$trans\text{-}RuCl_2(dmso–S)_4$	161[c]	
$cis\text{-}RuCl_2(dmso–S)_4$	148[a], 50[c], 190[c]	

[a] *trans* to Cl.
[b] *trans* to O.
[c] *trans* to S.

energy, especially when dmso–S is *trans* to dmso–O (from 161 to 208 kJ mol^{-1}). This is in agreement with the thermodynamic instability of the *trans* complex with respect to the *cis*,*fac* one, in part attributable to the competition for π electrons between *trans* dmso–S groups in the former [4]. This is also reflected by the binding energies in the hypothetical isomer *trans*-$RuCl_2(dmso–S)_3(dmso–O)$ which exhibits an even lower BE^S for the dmso–S *trans* to S (140 kJ mol^{-1}) and a higher BE^S for the dmso–S *trans* to O (230 kJ mol^{-1}). Finally, we can observe that in the hypothetical complex *cis*-$RuCl_2(dmso–S)_4$ the BE^S values are all lower than those of its linkage isomer *cis*,*fac*-$RuCl_2(dmso–S)_3(dmso–O)$ (Table 19). In fact, the all-S-bonded complex has never been detected, its total molecular energy being 56 kJ mol^{-1} higher than that of its linkage isomer [128].

The comparison of the coordination bond distances in *cis*,*fac*-$MCl_2(dmso–S)_3(dmso–O)$ (M = Os, Ru) showed that, while the Os–Cl and Os–O bond distances are, respectively, about 0.010 and 0.025 Å longer than the corresponding distances in the Ru derivative (in accord with the slightly larger covalent radius of osmium), the Os–S distances are about 0.008 Å shorter than the Ru–S distances [63]. The hypothesis of a strengthening of the metal to sulfur bonds in the osmium complex was confirmed by DFT B3LYP calculations of the M−dmso–S binding energy, BE^S, which is significantly greater for osmium (BE^S(Os)-BE^S(Ru) = 32.2, and 40.7 kJ mol^{-1}, for dmso–S *trans* to Cl, and dmso–S *trans* to O, respectively) [63]. The marked affinity of Os(II) for S-bonding is also shown by isolation of the complex *cis*-$OsCl_2(dmso–S)_4$, whose ruthenium analogue has never been detected.

The effect of ligands with different σ donor power, in determining the preference for S- and O-bonding, has been systematically examined in a series of hypothetical and real [*trans*-$MCl_4L(dmso)]^n$ complexes, with M = Ru(III) and Rh(III), and L = H^-, OH^-, Cl^- ($n = -2$), and NH_3, CO ($n = -1$) [126]. The different stability of the linkage isomers was evaluated from the difference between the total energies, $\Delta E^{O–S} = E^O - E^S$, calculated by the DFT B3LYP method, using a 6–31 G(d,p) basis for main group elements and an HW effective core potential for Ru and Rh [126]. It was shown that in all cases, in the gas phase, the S-bonded isomers are more stable than the O-isomers in the complexes, when L is a σ donor ligand ($45.6 < \Delta E^{O–S} < 64.5$ kJ mol^{-1} for M = Ru, $39.7 < \Delta E^{O–S} < 77.4$ kJ mol^{-1} for M = Rh). In the CO derivatives, the energy difference is markedly reduced, especially in the case of Ru(III) ($\Delta E^{O–S}$ = 8.11 kJ mol^{-1} for M = Ru, and 10.13 kJ mol^{-1} for M = Rh), so that interchange between the two linkage isomers is expected to become rather easy. $\Delta E^{O–S}$ increases with increase of the complex negative charge, *n*, and with the σ donor power of L ($H^- > OH^- > Cl^- > NH_3$) [126].

In addition, in order to get a measure of the coordination affinity of dmso towards the square pyramidal fragment $[MCl_mL_{5–m}]^n$, the M–dmso binding energies, BE^S and BE^O, for the dissociation process $[MCl_mL_{5–m}(dmso)]^n \rightarrow [MCl_mL_{5–m}]^n$ + dmso were calculated [126]. The properties of this fragment depend upon the nature of both M and L and should be responsible for the S- or O-bonding preference. DFT calculations have shown that there is a good correlation between $\Delta E^{O–S}$ (= BE^S–BE^O) and the absolute electronegativity (χ) of the five-coordinate fragment, while no definite trend was found for the global hardness (η) or softness ($S = 1/\eta$) [126]. As shown in Table 20, for M = Ru(III) χ markedly increases with *n*, passing from negative values when $n = -2$, to high positive values when $n = 1$. A similar trend has been calculated for Rh(III) complexes, suggesting that S-bonding is preferred when χ is less than about 2 eV. When χ is within 2–3 eV, the energy difference between the two linkage isomers is rather small and other factors (e.g. solvation, conformational entropy, steric hindrance) will determine the dmso bonding mode. Values of χ greater than 3 eV indicate a clear preference for O-bonding [126].

Table 20
Absolute electronegativity (χ, eV) and absolute hardness (η, eV) for the square pyramidal Ru(III) fragments $[RuCl_mL_{5–m}]^n$, together with $\Delta E^{O–S}$ (kJ mol^{-1}) and BE^O (kJ mol^{-1}) values

Complex	χ	η	$\Delta E^{O–S}$	BE^O
$[RuCl_4H]^{2-}$	−3.49	3.04	64.48	−9.42
$[RuCl_4(OH)]^{2-}$	−3.17	3.42	52.62	27.28
$[RuCl_5]^{2-}$	−2.23	3.15	50.69	35.21
$[RuCl_4(NH_3)]^-$	1.64	3.27	45.61	80.07
$[RuCl_4(CO)]^-$	2.57	3.09	8.11	66.48
$RuCl_3(CO)_2$	7.11	2.99	−45.94	141.75
$[RuCl_2(CO)_3]^+$	12.18	3.09	–[a]	245.74

[a] Not calculated for convergence problems [126].

3.5. Isomer equilibration

Thermodynamic parameters were calculated in the gas phase for the model isomerization process [*trans*-$RhCl_4(CO)(dmso–O)]^-$ → [*trans*-$RhCl_4(CO)$ (dmso–S)]$^-$ [126]. The slightly negative value calculated for ΔG_{298K} (−4.96 kJ mol^{-1}), shows again the slight preference for S-bonding, and possible equilibration of the two linkage isomers. Interestingly, the negative value of ΔS (−12.3 J mol^{-1} K^{-1}) is in agreement with the expected greater conformational flexibility of the dmso–O group, due to the greater number of degrees of freedom, with respect to dmso–S (see Section 4.1) [129]. Thus, from the conformational entropy point of view, the opposite isomerization process should be favored. In any case, in solution solvation effects can reverse the gas phase stability. In fact, DFT calculations have shown that for [*trans*-$RuCl_4(CO)(dmso)]^-$ polar solvents stabilize the O-isomer compared to the S-isomer (ca. 37 kJ mol^{-1} in acetone and ca. 34 kJ mol^{-1} in dmso) [126]. The Ru(III) dmso–O complex has been isolated from acetone and dmso solutions [130].

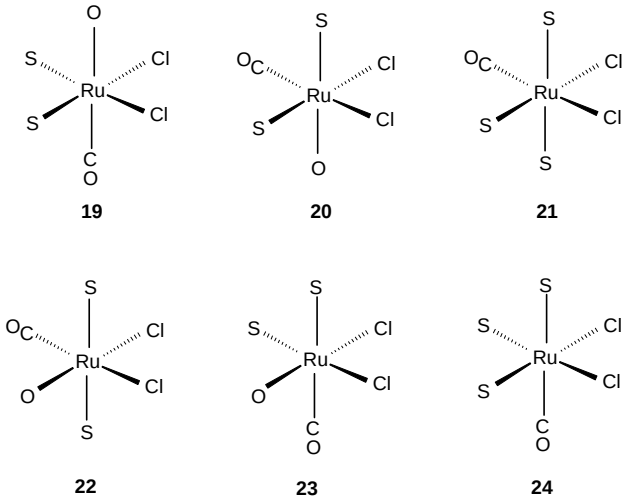

Scheme 7.

The relative stability of *cis*-$RuCl_2(dmso)_3(CO)$ isomers has been recently investigated by the DFT B3LYP method with a 6–31 G(d,p) basis for the main group elements and with the HW effective core potential for Ru [131]. Of the six possible isomers (**19**–**24**) (Scheme 7), in the gas phase, the two with dmso–S trans to CO (**23**, **24**) have the highest energies (>34 kJ mol^{-1}), while *cis*,*cis*,*cis*-$RuCl_2(dmso–S)_2(dmso–O)$ (CO) (**20**) exhibits the lowest energy, followed at a slightly higher energy (7.6 ± 0.7 kJ mol^{-1}) by *cis*,*mer*-$RuCl_2(dmso–S)_3(CO)$ (**21**) and *cis*,*trans*,*cis*-$RuCl_2(dmso–S)_2(dmso–O)$ (CO) (**22**). The isomer *cis*,*cis*,*trans*-$RuCl_2(dmso–S)_2(dmso–O)$ (CO) (**19**) is characterized by a moderately higher energy (18.4 kJ mol^{-1}). This trend is in fairly good agreement with the experimental observation that in chloroform solution, at room temperature, isomers **20** and **21** are approximately present in a 1:1 molar ratio (39% of **20**, 47% of **21**), while **19** is found in a lower percentage (19%), and **23** and **24** were not detected [131]. However, isomer **22**, which, according to the DFT calculations, has a molecular energy only 6.9 kJ mol^{-1} higher than that of **20**, was not observed in $CDCl_3$ solution [132]. Taking into account solvent effects, by means of the polarized continuum method, did not solve this discrepancy [131].

As a matter of fact, the evaluation of the equilibrium constants imply the much more complicated calculation of free energy differences. Such calculations were performed in an attempt to rationalize the equilibration processes between the three known isomers of the $OsCl_2(dmso)_4$ complex: *trans*-$OsCl_2(dmso–S)_4$ (**25**), *cis*,*fac*-$OsCl_2(dmso–S)_3(dmso–O)$ (**26**), and *cis*-$OsCl_2(dmso–S)_4$ (**27**) [63]. The electronic structures of the osmium complexes were calculated using the DFT B3LYP method with a 6–31 G(d,p) basis for main group elements, and with the HW effective core potential (ncore = 60) for the Os atom. ΔG_{298} values were calculated from the normal mode frequencies of the compounds in the gas phase on the basis of the adopted force field [63]. The gas phase molecular energies show small differences among the three isomers, in agreement with their observed equilibration. However, the lowest energy is exhibited by **25**, whereas, in $CHCl_3$ solution, at room temperature, this isomer is only a minor product (molar ratios, **25**:**26**:**27** = 1:33:66), in contrast also with the calculated (gas phase) equilibrium constants [63]. On the contrary, taking into account $CHCl_3$ and dmso solvation energies, the differences between the molecular energies are further reduced, and the new ΔG_{298} values (calculated applying the gas phase thermodynamic parameters) yield a population of **26** and **27** largely exceeding that of **25**. However, the calculated equilibrium constants are some orders of magnitude higher than the experimental ones [63]. In fact, an accurate isomer distribution analysis would imply the calculation of the normal mode frequencies in solution, and not simply in gas phase.

4. Empirical force-field investigations

4.1. Molecular mechanics

Molecular mechanics (MM) calculations were performed to investigate the role of steric interactions in determining the sulfoxide bonding mode in various ruthenium complexes [129,133–136]. In addition, in order to quantify the steric properties of sulfoxides, ‘cone angles’ were calculated for the most common sulfoxides, after minimization of their conformational energy using the program SYBYL and the TRIPOS 5.2 force field [129]. The results showed that the solid cone angles (Ω) and the corresponding circular cone apertures (Tolman cone angles, Θ) significantly increase from O- to S-bonded sulfoxides, in spite of the shorter metal-to-ligand distance assumed in the former case (M−O, 2.10 Å; M−S, 2.28 Å) [129].

The importance of the steric parameters was reflected by the isolation of different linkage isomers of Ru complexes depending on the sulfoxide bulkiness: while *mer*,*cis*-$RuCl_3(dmso–S)_2(dmso–O)$ is obtained in the case of dmso, the complex *mer*,*cis*-$RuCl_3(dpso–O)_2(dpso–S)$ (**28**) is obtained with the bulkier dpso ligand [129]. In order to investigate the effect of interligand steric interactions and find the most stable isomer, strain energies (E_{st}) were calculated for **28**, and for its possible isomers *mer*,*trans*-$RuCl_3(dpso–S)_2(dpso–O)$ (**29**), and *mer*,*cis*-$RuCl_3(dpso–S)_2(dpso–O)$ (**30**). Conformational analyses were carried out with the program SYBYL and the TRIPOS 5.2 force field (no electrostatic interactions), after implementation with the Ru(III) parameters estimated from spectroscopic data combined with the Badger’s and Halgren’s equations [129]. The MM calculations showed that the strain energy increases from **28** to **30** ($E_{st} = -81.2$ (**28**), −72.4 (**29**), −54.0 (**30**) kJ mol^{-1}), with a large difference between the two linkage isomers **28** and **30** ($\Delta E_{st} = 27.2$ kJ mol^{-1}). It was also observed that in the

three isomers there were large differences in the number of low-energy conformers, indicating a noticeable difference of conformational entropy, S_{co}, again in favor of isomer **28** (S_{co} = 9.7 (**28**), 5.2 (**29**), 4.5 (**30**) J mol^{-1} K^{-1}). The difference ($E_{st} - TS_{co}$) was taken as a measure of the global interligand steric interactions, combining strain and conformational entropy terms. At T = 298 K, the (E_{st}–TS_{co}) differences between isomers **28** and **29**, and **28** and **30** are of 31.8 and 53.6 kJ mol^{-1}, respectively, confirming a strong preference for **28**, the complex found in solution and in the solid state [129].

MM calculations were also used for a rationalization of the stereochemical and conformational behavior of Ru(II)–dmso complexes containing aromatic nitrogen ligands (L) of general formula *cis*,*cis*,*cis*-$RuCl_2$(dmso–S)$_2$(L1) (L2) (**31**) [133]. Calculations were performed using the program HYPERCHEM 4.5 and the AMBER force field, in which the force field constants involving the Ru(II)(Cl) (L) (dmso) groups were calculated from the Badger's and Halgren's equations, after optimization (Simplex method) of the related parameters, on the basis of 11 accurate crystal structures [133]. For the electrostatic contribution, atomic charges were calculated by the semi-empirical ZINDO/1 method. The consistency of the force field obtained is shown by the root-mean-square deviations between observed and calculated bond lengths and angles, of 0.017 Å and 1.3°, respectively, for the whole set of data, and of 0.013 Å and 1.6°, respectively, for the ruthenium parameters. The force field was first used to analyze the rotational freedom around the Ru–S, Ru–O and S–O bonds in *cis*,*fac*-$RuCl_2$(dmso–S)$_3$(dmso–O). As to the rotation around the Ru–S bond, the profile of the strain energy as a function of the S–Ru–S–O torsion angle (ψ) shows two lowest minima at $\psi = \pm 80°$ and three other minima, at an energy 13.4 kJ mol^{-1} higher, at $\psi = -5$, 25, and 180° [133]. This is consistent with the observation that this complex has been isolated, in the solid state, as three polymorphs with ψ = 9.2° (**F1**), 11.7° (**F2**), and −70.5° (**F3**), the last one being the thermodynamically most stable [133]. Rotation around the Ru–O bond, measured by the Cl–Ru–O–S torsion angle, is much less hindered, being characterized by a rather flat E_{st} minimum between −120 and 40° [133]. Finally, the profile of E_{st} versus the Ru–O–S–C torsion angle shows that the absolute minimum occurs for the most common *trans–trans* conformation, while higher energy minima correspond to the *cis–trans* and *cis–cis* conformations, in agreement with their less frequent observed occurrence [4].

As to restricted rotation of nitrogen bases, two E_{st} minimum structures were calculated for *cis*,*cis*,*cis*-$RuCl_2$(dmso–S)$_2$(dmim) (dmpy) (**31**) corresponding to two opposite orientations of the dmpy ligand. This is in agreement with the fluxional behavior detected in solution, and the crystal structure of **31**, characterized by a molecular static disorder of the dmpy ligand, with two orientations at 180° to each other. Moreover, for *cis*,*cis*,*cis*-$RuCl_2$(dmso–S)$_2$(dmim)$_2$, four rotamers were detected in solution [137], in correspondence to the four E_{st} minima in gas phase [133].

The mutual orientation of two *cis* dmso–S groups has been analyzed in detail in the NMR and MM study of Ru(II) octahedral complexes of formula RuX_2(dmso–S)$_{2-n}$(CO)$_n$(L1) (L2) (X = Cl, Br; n = 0–1; L1, L2 = lopsided imidazole-like ligands), with both *cis* and *trans* X arrangements [135]. For the *cis*,*cis*,*cis*-RuX_2(dmso–S)$_2$(L1) (L2) complexes (**32**), the head-to-head (HH) and head-to-tail (HT) descriptors, with the 'up' (u) and 'down' (d) specification, used to define the mutual orientation of the N-ligands, were used also for the dmso–S ligands [135] (Scheme 8).

Considering the dmso O atom as the ligand 'head', the $(HH)_u$ or the $(HH)_d$ conformations are possible, if both torsion angles O–S–Ru–S (ψ) are, respectively, in the range 0° < ψ < 180° or −180° < ψ < 0° (Δ enantiomer). For a more precise definition of the orientation of the two pairs of *cis* ligands the $H_{\psi a}H_{\psi b}$ and $H_{\psi c}H_{\psi d}$ notation has been introduced (in the scheme, *a* and *b* are the positions taken by the N ligands, while *c* and *d* are those taken by the dmso's), together with the simpler H_iH_j notation, where i and j (i, j = 1–4) refer to the quadrants of the torsion angles ψ [135]. In all known crystal

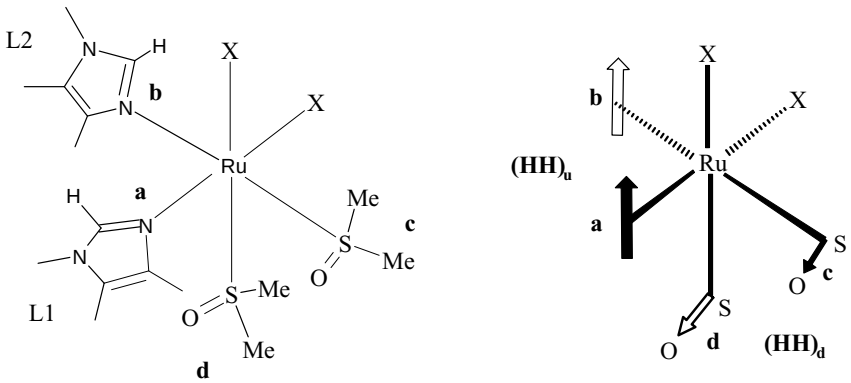

32

Scheme 8.

structures, the Δ *cis*,*cis*,*cis*-$RuX_2(dmso–S)_{2-n}(CO)_n(L1)$ (L2) complexes adopt the $(HH)_d$ conformation for the dmso ligands with average values for ψ_c and ψ_d of -14 ± 12 and $86 \pm 6°$, respectively. This conformation corresponds to structures in which the O atom of each dmso group lies approximately in the coordination plane perpendicular to the Ru–S bond of the other dmso ligand, with the methyl groups of each dmso stradling one *cis* Ru–X bond. Similar conformations were found in the minimum strain energy structures of *cis*,*cis*,*cis*-$RuCl_2(dmso–S)_2(tmbim)_2$ and *cis*,*cis*,*cis*-$RuCl_2(dmso–S)_2(dmim)$ (tmbim) [135].

Unlike in the *cis*,*cis*,*cis* complexes, the solid state conformation of the two *cis* dmso–S ligands in the *trans*,*cis*,*cis*-$RuX_2(dmso–S)_2(L1)$ (L2) complexes is HT, with ψ values of about 31 and 161°, close to the minimum strain energy values of 24 and 169°.

In this conformation, the two O atoms are significantly displaced from the RuS_2 plane (ca. ±0.45 Å). However, the MM calculations indicate that the energy difference between these HT arrangements and the 'planar' (PP) arrangement (both O atoms in the Ru–S_2 plane) is very small ($0.4\,kJ\,mol^{-1}$). In fact, a strictly symmetry-determined PP geometry of pairs of *cis* dmso–S ligands has been observed in *trans*-$MX_2(dmso–S)_4$ complexes (M = Ru, Os; X = Cl, Br) [4].

The relative orientation of three *fac* dmso–S groups was examined by a conformational analysis of the [*fac*-$RuCl_3(dmso–S)_3]^-$ complex, using the previously described force field [136]. The conformation of the three dmso–S ligands is described by the dihedral angle (α) between the planes defined by the O and S atoms, and by the pseudo-torsion angles around the Ru−S bonds, $\phi_i = O_i–S_i–Ru–S^*$ (i = 1–3; S* = midpoint of the three S atoms). The MM calculations show that the minimum strain energy structure corresponds to the rotamer with $\alpha = 0°$ and $\phi_1 = \phi_2 = \phi_3 = 27.8°$. In fact, similar geometries were found in all the crystal structures of the [*fac*-$RuX_3(dmso–S)_3]^-$ (X = Cl, Br) complex ($0.3° < \alpha < 3.3°$, $25.8° < \phi < 29.3°$) [136]. When the pseudo C_3 symmetry is removed, as in *cis*,*fac*-$RuCl_2(dmso–S)_3(dmso–O)$, the lowest calculated energy is found for the rotamer with $\alpha = 25.8°$, $\phi_1 = 133.7°$, $\phi_2 = 38.5°$, and $\phi_3 = 16.5°$, in agreement with the values of $\alpha = 24.2°$, $\phi_1 = 118.7°$, $\phi_2 = 55.9°$, and $\phi_3 = 14.2°$, found in the thermodynamically most stable polymorph **F3** (see above). The values found in the other two polymorphs, **F1** and **F2**, are close to the values calculated for the higher energy conformer ($\Delta E = 5.4\,kJ\,mol^{-1}$), with $\alpha = 2.7°$, $\phi_1 = 21.3°$, $\phi_2 = 31.7°$, and $\phi_3 = 37.4°$.

The same force field was also used, after implementation for new bond angle parameters, for a stereochemical analysis of ruthenium bis-chelate disulfoxide complexes of formula $RuCl_2(bmse)_2$ (**34**) [134]. The aim of this work was the study of the influence of non-bonded atom interactions, arising from linkage and *cis–trans* isomerism combined with different arrangements of the sulfur chiral centers,

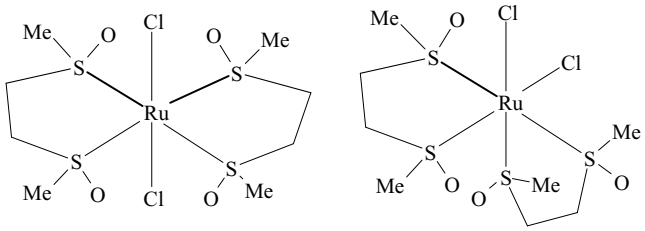

35 **36**

Scheme 9.

on the strain energy of the compounds. The MM analysis was restricted to the four most likely stereoisomers of **34**: *trans*-$RuCl_2(bmse-S,S)_2$ (**35**), *cis*-$RuCl_2(bmse-S,S)_2$ (**36**), *trans*-$RuCl_2(bmse–S,O)_2$ (**37**), and *cis*-$RuCl_2(bmse-S,S)$ (bmse–S,O) (**38**), in which bmse represent both *meso* and *rac* ligands. These 4, out of the 17 envisageable stereoisomers, are expected to be the most stable from the electronic point of view and do not contain the less probable seven-membered rings, formed in the case of O,O chelation [134] (Schemes 9 and 10).

The MM results show that for each diastereomer **35**, **36**, **37**, and **38**, the strain energy is markedly dependent on the environment of the chiral center, mainly because of the electrostatic energy terms. In fact, the change of chirality of the sulfur atoms implies a different orientation of the negatively charged oxygen atoms and correspondingly of the positively charged methyl groups.

In the case of the *cis* isomers **36** and **38**, containing *meso*-bmse, the lowest strain energy is calculated for the isomer of type **36** with *trans* sulfur atoms of the same chirality, as in the case of the diastereomer 33-$[RuCl_2S_4]$ Δ (according to the IUPAC stereochemical descriptors) (**39**) [134]. This same structure was found in the solid state for *cis*-$RuCl_2(bese-S,S)_2$, whose crystals contain the enantiomeric pair 33-$[RuCl_2S_4]$ Δ and 22-$[RuCl_2S_4]$ Λ [138]. All other isomers, of both types **36** and **38**, have significantly higher strain energies ($\Delta E_{st} > 58.6\,kJ\,mol^{-1}$). For the *trans* isomers **35** and **37**, the lowest energy is calculated for the diastereomer 13-$[RuCl_2S_4]$ of type **35**, that is for the isomer with sulfur atoms of opposite chirality *trans* to each other (**40**). Interestingly, analogous stereomers were observed in the crystal structures of both *trans*-$RuCl_2(bmse)_2$ and *trans*-$RuCl_2(bpse)_2$ [138].

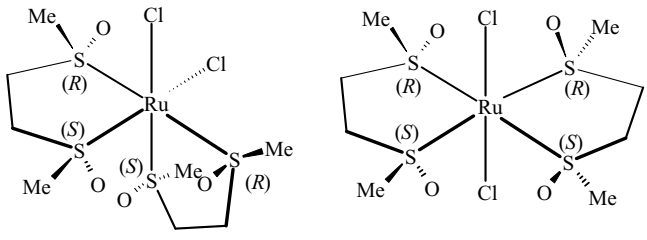

39 **40**

Scheme 10.

Using the *rac*-bmse ligand, MM calculations predict that the lowest strain energy would be found for 32-[$RuCl_2S_4$] Δ (type **36**), for the *cis* isomers, and for 12-[$RuCl_2S_4$] (type **35**) for the *trans* isomers [134]. Finally, in both *cis* and *trans* isomers, the passage from S,S to S,O bonding, that is, from five- to six-membered rings, implies a significant increase of the strain energies.

4.2. Molecular dynamics

Molecular dynamic (MD) simulations of pure dmso and its 'inifinitely diluted solutions' of Na^+ and Cl^- were performed at 298.15 K using the VG force field [114]. Each ion was considered separately in a NVT ensemble of 215 dmso molecules. It is found that the first solvation shell of Na^+ consists of six dmso molecules located at the vertices of a distorted octahedron and oriented by their polar S–O bonds towards the cation with a preferable angle of 156° between S–O and Na–S vectors. The radial distribution function (RDF) of Na^+ exhibits an intense first peak corresponding to the Na···O distance of 2.4 Å, and a second lower peak at 3.7 Å for Na···S. Translational and reorientational mobilities of the coordinated dmso molecules are significantly lower than in bulk solvent. On the contrary, the first solvation shell of Cl^- does not correspond to a regular polyhedron. It consists of 10 dmso molecules oriented by their methyl groups and sulfur atoms towards the anion with a preferential angle of 90° between the bisector of the C–S–C bond angle and the vector pointing from Cl^- to the midpoint of the two methyl groups. The dynamic behavior of these dmso molecules is similar to that of the solvent molecules in the bulk. The RDFs of the closest interaction sites ($Na^+\cdots O$, $Cl^-\cdots C$) show broad second peaks at 6.8 and 7.6 Å, respectively, with almost similar intensities. This shows that second solvation shells can be identified in both cases, but they are not so well defined as the first solvation shells.

For references concerning MD calculations for pure dmso, and dmso mixtures with water, bio-molecules and electrolytes see [139].

5. Conclusions

The statistical analysis of the sulfoxide S–O bond distances, obtained through accurate X-ray diffraction analyses, shows a significant variation between free and metal coordinated sulfoxides. In fact, from the 119 (n) values available for free sulfoxides (pure and solvate compounds), the semi-weighted mean ($\langle x\rangle_s$) (with standard error in brackets) is 1.492(1) Å, 98% of the values lying within 1.4900 and 1.4944 Å. In the S-bonded metal complexes $\langle x\rangle_s$ reduces to 1.4738(7) Å (n = 474, 98% of values in the range 1.4716–1.4746 Å), while in the O-bonded metal complexes $\langle x\rangle_s$ is increased to 1.528(1) Å (n = 291, 98% of values in the range 1.5250–1.5300 Å). When the oxygen atom of uncoordinated sulfoxides is involved in hydrogen bonds, the mean S–O bond distance increases from 1.492(1) Å to 1.513(2) Å, with 98% of the 27 available data lying within 1.5085 and 1.5177 Å. The S–O bond length is further increased by O protonation to give preferentially the $[(\text{sulfoxide–O})_2H]^+$ species, in which $\langle x\rangle_s$ = 1.541(3) Å (n = 12, 98% of values in the range 1.5334–1.5470 Å). The longest S–O distances were found in two $[(\text{sulfoxide–O})H]^+$ cations, 1.585(8) Å for dmso and 1.589(3) Å for tmso. The trend of the S–O bond lengths is fully consistent with the changes of the dmso SO stretching frequency upon coordination. In fact, for dmso, ν(SO) is found in the range 1036–1070 cm^{-1} (condensed phase), while it lies in the range 1080–1154 cm^{-1} in S-bonded metal complexes, and in the range 862–997 cm^{-1} in O-bonded metal complexes. The weakening of the S–O bond upon O-coordination and its strengthening upon S-coordination is also confirmed by quantum chemical investigations, which include the calculation of S–O stretching frequencies and bond lengths.

The calculation of the metal−dmso binding energies, based on DFT methods, provide indications about the linkage isomer stability, showing a general preference for S-bonding, in the absence of π-acceptor ligands, in agreement with the experimental evidence.

In the case of the octahedral $[MCl_mL_{5-m}(\text{dmso})]^n$ complexes (M = Ru(III), Rh(III); $0 \le m \le 5$; $-2 \le n \le 2$), a good correlation has been found between the absolute electronegativity of the five-coordinate square pyramidal fragment $[MCl_mL_{5-m}]^n$ and the energy difference between the dmso–S and dmso–O linkage isomers, ΔE^{O-S}. It was found that χ increases with the increase of n and the decrease of the σ-donor power of L. The comparison of the ΔE^{O-S} values with the observed isomer stability has suggested that S-bonding is highly preferred when $\chi < 2$ eV, while O-bonding is preferred when $\chi > 3$ eV. In the intermediate cases the isomer energy difference is small and the dmso binding mode may be essentially determined by steric and/or solvation effects. In fact, it has been found that the correct calculation of the equilibrium constants, for the isomer equilibration, requires an accurate calculation of the solvation energies.

Future work requires the calculation of the normal mode frequencies of the compounds in solution (and not simply in the gas phase), as well as the calculation of the metal electronegativity (χ_M) (instead of the fragment electronegativity, χ) to be related to ΔE^{O-S}, as a function of the σ/π L donor power. Inclusion of nitrosyl complexes should be of particular interest, to confirm the marked preference for O-bonding observed in Ru–NO complexes.

Molecular mechanics calculations have shown the importance of intramolecular non-bonded atom interactions in determining the S/O bonding mode, because of the different steric effects of O- and S-bonded sulfoxides. These are also responsible for the mutual orientation of the dmso ligands, and control the ligand rotation about the coordination bonds. For dmso, rotation is rather free in O-bonded

complexes, while it is much more restricted in S-bonded complexes. This indicates that, in the absence of definite electonic factors, O-bonding is favored by a steric entropy factor. The structural characterization of enantiomerically pure chiral disulfoxide complexes appears of interest to complete the investigation of the influence of the sulfur atom chiralities on the metal complex structure, which, in turn, can determine interesting chemical and biological properties.

Note added in proofs

After submission of the paper, S. Geremia determined the crystal structure of pure dmso at 164 K ($R = 4.0\%$, 767 reflections with $1 > 2\sigma(I)$ over a total of 955). The S–O distance is of 1.480(2) Å. Inspection of the anisotropic thermal parameters shows that the distance can be shortened by thermal motion effects. After correction the distance is of 1.499 Å.

Acknowledgements

The author is grateful to all those who contributed to this work. This work was financially supported by MIUR.

References

[1] J.A. Davies, Adv. Inorg. Chem. Radiochem. 24 (1981) 115.
[2] H.B. Kagan, B. Ronan, Rev. Hetero. Chem. 7 (1992) 92.
[3] V.Y. Kukushkin, Coord. Chem. Rev. 139 (1995) 375.
[4] M. Calligaris, O. Carugo, Coord. Chem. Rev. 153 (1996) 83.
[5] M. Calligaris, Croat. Chem. Acta 72 (1999) 147.
[6] E. Alessio, Coord. Chem. Rev., to be published.
[7] F.A. Cotton, E.V. Dikarev, M.A. Petrukhina, S.-E. Stiriba, Inorg. Chem. 39 (2000) 1748.
[8] R. Thomas, C.B. Shoemaker, K. Eriks, Acta Crystallogr. 21 (1966) 12.
[9] M. Bakir, Acta Crystallogr. C57 (2001) 1154.
[10] A.J. Blake, M. Felloni, P. Hubberstey, M. Schröder, C. Wilson, Acta Crystallogr. C57 (2001) m556.
[11] J. Drabowicz, B. Dudziński, M. Mikołajczyk, M.W. Wieczorek, W.R. Majzner, Tetrahedron: Asymmetry 9 (1998) 1171.
[12] A.V. Yatsenko, S.V. Medvedev, A.I. Tursina, L.A. Aslanov, Zh. Obs. Khim. 56 (1986) 2330.
[13] D. Casarini, L. Lunazzi, A. Mazzanti, Angew. Chem. Int. Ed. 40 (2001) 2536.
[14] D. Casarini, S. Grilli, L. Lunazzi, A. Mazzanti, J. Org. Chem. 66 (2001) 2757.
[15] P. Bravo, E. Corradi, M. Crucianelli, S.V. Meille, M. Zanda, Acta Crystallogr. C55 (1999) 687.
[16] D.R. Evans, M. Huang, W.M. Seganish, J.C. Fettinger, T.L. Williams, Inorg. Chem. Commun. 6 (2003) 462.
[17] M. Calligaris, A. Melchior, S. Geremia, Inorg. Chim. Acta 323 (2001) 89.
[18] S.R. Bennett, A.R. Kennedy, A.I. Khalaf, R.D. Waigh, Acta Crystallogr. C54 (1998) 1511.
[19] P.-H. Leung, A. Liu, K.F. Mok, A.J.P. White, D.J. Williams, J. Chem. Soc., Dalton Trans. (1999) 1277.
[20] P. Kumaradhas, N. Kalyanon, K. Ravikumar, K.C. Mohan, M.A. Sridhar, J.S. Prasad, K.A. Nirmala, Acta Crystallogr. C55 (1999) 614.
[21] J.K. Harper, N.K. Dalley, A.E. Mulgrew, F.G. West, D.M. Grant, Acta Crystallogr. C57 (2001) 64.
[22] A.C. Blackburn, L.J. Fitzgerald, R.E. Gerkin, Acta Crystallogr. C53 (1997) 1991.
[23] A.D. Bond, Acta Crystallogr. E58 (2002) o194.
[24] D. Cannon, J.N. Low, J. Cobo, S. Molina, M. Nogueras, A. Sánchez, C. Glidwell, Acta Crystallogr. C57 (2001) 608.
[25] R.D. Gilardi, R.J. Butcher, Acta Crystallogr. E57 (2001) o757.
[26] K. Wijaya, O. Moers, A. Blaschette, P.G. Jones, Acta Crystallogr. C54 (1998) 1707.
[27] D. Tranqui, P. Fresneau, M. Cussac, Acta Crystallogr. C54 (1998) 1501.
[28] B.R. James, R.H. Morris, F.W.B. Einstein, A. Willis, J. Chem. Soc., Chem. Commun. (1980) 31.
[29] B. Viossat, P. Khodadad, N. Rodier, J. Mol. Struct. 71 (1981) 237.
[30] E. Alessio, B. Milani, G. Mestroni, M. Calligaris, P. Faleschini, W.M. Attia, Inorg. Chim. Acta 177 (1990) 255.
[31] L. Messori, G. Marcon, P. Orioli, M. Fontani, P. Zanello, A. Bergamo, G. Sava, P. Mura, J. Inorg. Biochem. 95 (2003) 37.
[32] R.S. Srivastava, F.R. Fronczek, Inorg. Chim. Acta 322 (2001) 32.
[33] D. Hesek, Y. Inoue, S.R.L. Everitt, H. Ishida, M. Kunieda, M.G.B. Drew, J. Chem. Soc., Dalton Trans. (1999) 3701.
[34] Y. Yamamoto, K. Sugawara, T. Aiko, J.-F. Ma, J. Chem. Soc., Dalton Trans. (1999) 4003.
[35] W. Levason, S.D. Orchard, G. Reid, J. Chem. Soc., Dalton Trans. (2000) 4550.
[36] M. Biagini Cingi, M. Lanfranchi, M.A. Pellinghelli, M. Tegoni, Eur. J. Inorg. Chem. (2000) 703.
[37] P. Satyanarayan, P. Samudranil, Acta Crystallogr. C58 (2002) m273.
[38] M.F.C. Guedes da Silva, A.J.L. Pombeiro, S. Geremia, E. Zangrando, M. Calligaris, A.V. Zinchenko, V. Y. Kukushkin, J. Chem. Soc., Dalton Trans. (2000) 1363.
[39] J. Rusanova, E. Rusanov, A.B.P. Lever, private communication.
[40] J.J. Rack, J.R. Winkler, H.B. Gray, J. Am. Chem. Soc. 123 (2001) 2432.
[41] C. Sens, M. Rodríguez, I. Romero, A. Llobet, T. Parella, B.P. Sullivan, J. Benet-Buchholz, Inorg. Chem. 42 (2003) 2040.
[42] P.M.T. Piggot, L.A. Hall, A.J.P. White, D.J. Williams, Inorg. Chim. Acta 357 (2004) 207.
[43] P.M.T. Piggot, L.A. Hall, A.J.P. White, D. J. Williams, Inorg. Chim. Acta, in press.
[44] E. Rüba, C. Gemel, C. Slugovc, K. Mereietr, R. Schmid, K. Kirchner, Organometallics 18 (1999) 2275.
[45] K. Jitsukawa, H. Shiozaki, H. Masuda, Tetrahedron Lett. 43 (2002) 1491.
[46] T. Clark, J. Cochrane, S.F. Colson, K.Z. Malik, S.D. Robinson, J.W. Steed, Polyhedron 20 (2001) 1875.
[47] A.K. Singh, M. Kadarkaraisamy, J.E. Drake, R.J. Butcher, Inorg. Chim. Acta 304 (2000) 45.
[48] W. Levason, S.D. Orchard, G. Reid, J. Chem. Soc., Dalton Trans. (2000) 4550.
[49] L. Otero, P. Noblia, D. Gambino, H. Cerecetto, M. Gonzáles, J.A. Ellena, O.E. Piro, Inorg. Chim. Acta 344 (2003) 85.
[50] C. Gemel, K. Folting, K.G. Caulton, Inorg. Chem. 39 (2000) 1593.
[51] T. Kojima, T. Amano, Y. Ishii, M. Ohba, Y. Okaue, Y. Matsuda, Inorg. Chem. 37 (1998) 4076.
[52] G. Delgado, A.V. Rivera, T. Suárez, B. Fontal, Inorg. Chim. Acta 233 (1995) 145.
[53] A. Garas, D.C. Craig, R.S. Vagg, A.T. Baker, J. Coord. Chem. 50 (2000) 79.
[54] S.F. Lessing, S. Lotz, H.M. Roos, P.H. van Rooyen, J. Chem. Soc., Dalton Trans. (1999) 1499.
[55] M. Otto, J. Parr, A.M.Z. Slawin, Organometallics 17 (1998) 4527.
[56] J.J. Rack, H.B. Gray, Inorg. Chem. 38 (1999) 2.

[57] I. Turel, M. Pečanac, A. Golobič, E. Alessio, B. Serli, Eur. J. Inorg. Chem. (2002) 1928.
[58] B. Serli, E. Iengo, T. Gianferrara, E. Zangrando, E. Alessio, Metal Based Drugs 8 (2001) 9.
[59] C. Price, M.A. Shipman, S.L. Gummerson, A. Houlton, W.Clegg, M.R.J. Elsegood, J. Chem. Soc., Dalton Trans. (2001) 353.
[60] C. Price, M.R.J. Elsegood, W. Clegg, N.H. Rees, A. Houlton, Angew. Chem. Int. Ed. Engl. 36 (1997) 1762.
[61] Q.A. de Paula, A.A. Batista, O.R. Nascimento, A.J. da Costa-Filho, M.S. Schultz, M.R. Bonfadini, G. Oliva, J. Braz. Soc. 11 (2000) 530.
[62] R.C. van der Drift, J.W. Sprengers, E. Bouwman, W.P. Mul, H. Kooijman, A.L. Spek, E. Drent, Eur. J. Inorg. Chem. (2002) 2147.
[63] E. Alessio, B. Serli, E. Zangrando, M.Calligaris, N.S. Panina, Eur. J. Inorg. Chem. (2003) 3160.
[64] R. Dorta, H. Rozenberg, D. Milstein, Chem. Commun. (2002) 710.
[65] N.N. Sveshnikov, M.H. Dickman, M.T. Pope, Acta Crystallogr. C56 (2000) 1193.
[66] E. Fooladi, T. Graham, M.L. Turner, B. Dalhus, P.M. Maitlis, M. Tilset, J. Chem. Soc., Dalton Trans. (2002) 975.
[67] R. Dorta, H. Rozenberg, L.J.W. Shimon, D. Milstein, J. Am. Chem. Soc. 124 (2002) 188.
[68] M.H. Johansson, Å. Oskarsson, Acta Crystallogr. C57 (2001) 1265.
[69] C. Pettinari, M. Pellei, G. Cavicchio, M. Crucianelli, W. Panzeri, M. Colapietro, A. Cassetta, Organometallics 18 (1999) 555.
[70] R. Cini, A. Donati, R. Giannettoni, Inorg. Chim. Acta 315 (2001) 73.
[71] C. Sacht, M.S. Datt, S. Otto, A. Roodt, J. Chem. Soc., Dalton Trans. (2000) 4579.
[72] P.S. Fontes, Å. Oskarsson, K. Lövqvist, N. Farrell, Inorg. Chem. 40 (2001) 1745.
[73] G.M. Arvanitis, C.E. Holmes, D.G. Johnson, M. Berardini, Acta Crystallogr. C56 (2000) 1332.
[74] J. Bruce, D. Johnson, W. Cordes, R. Sadoski, J. Chem. Crystallogr. 27 (1997) 695.
[75] P. Nilsson, O.F. Wendt, Acta Crystallogr. E58 (2002) m639.
[76] R.M. Dyksterhouse, B.A. Howell, P.J. Squattrito, Acta Crystallogr. C56 (2000) 64.
[77] A.D. Ryabov, G.M. Kazankov, I.M. Panyashkina, O.V. Grozovsky, O.G. Dyachenko, V.A. Polyakov, L.G. Kuz'mina, J. Chem. Soc., Dalton Trans. (1997) 4385.
[78] T.A.K. Al-Allaf, L.J. Rashan, A.S. Abu-Surrah, R. Fawzi, M. Steimann, Trans. Met. Chem. 23 (1998) 403.
[79] O. Kristiansson, P. Lindqvist-Reis, Acta Crystallogr. C56 (2000) 163.
[80] M. Klinga, R. Cuesta, J.M. Moreno, J.M. Dominguez-Vera, E. Colacio, R. Kivekas, Acta Crystallogr. C54 (1998) 1275.
[81] W.J. Oldham, B.L. Scott, K.D. Abney, W.H. Smith, D.A. Costa, Acta Crystallogr. C58 (2002) m139.
[82] S. Kannan, S. Shanmuga Sundara Raj, H.-K. Fun, Acta Crystallogr. C56 (2000) e545.
[83] X.Q. Wang, W.T. Y, D. Xu, M.K. Lu, D.R. Yuan, Acta Crystallogr. C56 (2000) 418.
[84] M. Otto, B.J. Boone, A.M. Arif, J.A. Gladysz, J. Chem. Soc., Dalton Trans. (2001) 1218.
[85] J.-R. Tzou, M. Mullaney, R.E. Norman, S.-C. Chang, Acta Crystallogr. C51 (1995) 2249.
[86] E. Zangrando, B. Serli, L. Yellowlees, E. Alessio, J. Chem. Soc., Dalton Trans. (2003) 4391.
[87] X.-P. Hu, X.-L. Feng, J. Cai, L.-N. Ji, Acta Crystallogr. C56 (2000) e388.
[88] M. Nonoyama, K. Nakajima, Polyhedron 18 (1999) 533.
[89] L. Casella, O. Carugo, M. Gullotti, S. Dolci, M. Frassoni, Inorg. Chem. 35 (1996) 1101.
[90] R. Wang, M. Hong, Y. Liang, R. Cao, Acta Crystallogr. E57 (2001) m277.
[91] J. Drabowicz, B. Dudziński, M. Mikołajczyk, F. Wang, A. Dehlavi, J. Goring, M. Park, C.J. Rizzo, P.L. Polavarapu, P. Biscarini, M.W. Wieczorek, W.R. Majzner, J. Org. Chem. 66 (2001) 1122.
[92] A.V. Ytsenko, S.V. Medvedev, L.A. Aslanov, Koord. Khim. 17 (1991) 1338.
[93] S. Mandolesi, M. Studentkowski, H. Preut, T. Mitchell, Acta Crystallogr. E57 (2001) m543.
[94] S.W. Ng, Acta Crystallogr. C54 (1998) 745.
[95] G.F. de Sousa, C.A.L. Filgueiras, J.F. Nixon, P.B. Hitchcock, J. Braz. Chem. Soc. 8 (1997) 649.
[96] R. Taylor, O. Kennard, Acta Crystallogr. B39 (1983) 517.
[97] (a) D.L. Massart, B.G.M. Vandeginste, L.M.C. Buydens, S. De Jong, P.J. Lewi, J. Smeyers-Verbeke, Handbook of Chemometrics and Qualimetrics: Part A, Elsevier, Amsterdam, 1997, p. 58;
(b) D.L. Massart, B.G.M. Vandeginste, L.M.C. Buydens, S. De Jong, P.J. Lewi, J. Smeyers-Verbeke, Handbook of Chemometrics and Qualimetrics: Part A, Elsevier, Amsterdam, 1997, p. 60;
(c) D.L. Massart, B.G.M. Vandeginste, L.M.C. Buydens, S. De Jong, P.J. Lewi, J. Smeyers-Verbeke, Handbook of Chemometrics and Qualimetrics: Part A, Elsevier, Amsterdam, 1997, p. 63;
(d) D.L. Massart, B.G.M. Vandeginste, L.M.C. Buydens, S. De Jong, P.J. Lewi, J. Smeyers-Verbeke, Handbook of Chemometrics and Qualimetrics: Part A, Elsevier, Amsterdam 1997, p. 116
[98] M. Mikuriya, M. Fukuya, Bull. Chem. Soc. Jpn. 69 (1996) 679.
[99] N.-O. Björk, A. Cassel, Acta Chem. Scand. A30 (1976) 235.
[100] M. Nieuwenhuyzen, C.J. Wilkins, J. Chem. Soc., Dalton Trans. (1993) 2673.
[101] H. Schmidbaur, H.-J. Öller, D.L. Wilkinson, B. Huber, G. Müller, Chem. Ber. 122 (1989) 31.
[102] P. Biscarini, L. Fusina, G.D. Nivellini, A. Mangia, G. Pelizzi, J. Chem. Soc., Dalton Trans. (1974) 1846.
[103] M. Tschinkl, A. Schier, J. Riede, F.P. Gabbai, Angew. Chem. Int. Ed. 38 (1999) 3547.
[104] T.J. Karol, J.P. Hutchinson, J.R. Hyde, H.G. Kuivila, J.A. Zubieta, Organometallics 2 (1983) 106.
[105] T. Tanase, T. Aiko, Y. Yamamoto, Chem. Commun. (1996) 2341.
[106] S. Geremia, S. Mestroni, M. Calligaris, E. Alessio, J. Chem. Soc., Dalton Trans. (1998) 2447.
[107] S. Geremia, M. Calligaris, S. Mestroni, Inorg. Chim. Acta 292 (1999) 144.
[108] M.-T. Forel, M. Tranquille, Spectrochim. Acta A26 (1970) 1023.
[109] S. Bianco, R.S. Cataliotti, S. Chieli, F. Guerrini, C. Gaburri, G. Paliani, A. Peraio, M. Scamosci, C. Schioppa, C. Taratza, Spectrochim. Acta A42 (1986) 855.
[110] H. Torii, M. Tasumi, Bull. Chem. Soc. Jpn. 68 (1995) 128.
[111] F. Tureèek, J. Phys. Chem. A102 (1998) 4703.
[112] W. Feder, H. Dreizler, H.D. Rudolph, V. Typke, Z. Naturforsch, Teil A 24 (1969) 266.
[113] L.C. Jitariu, C. Wilson, D.M. Hirst, J. Mol. Struct. (Theochem.) 391 (1997) 111.
[114] O.N. Kalugin, M.N. Volobuev, A.V. Ishchenko, A.K. Adya, J. Mol. Liq. 91 (2001) 135.
[115] T.F. Magnera, G. Caldwell, J. Sunner, S. Ikuta, P. Kebarle, J. Am. Chem. Soc. 106 (1984) 6140.
[116] G.A. Olah, D.J. Donovan, H.C. Lin, H. Mayr, P. Andreozzi, G. Klopman, J. Org. Chem. 43 (1978) 2268.
[117] A. Bagno, G. Scorrano, J. Phys. Chem. 100 (1996) 1536.
[118] G. Rasul, G.K.S. Prakash, G.A. Olah, J. Org. Chem. 65 (2000) 8786.
[119] S.V. Dozmorov, Zh. Prikl. Spektrosk. 45 (1986) 438.
[120] N.S. Panina, Y.N. Kukushkin, Zh. Neorg. Khim. 43 (1998) 88; N.S. Panina, Y.N. Kukushkin, Russ. J. Inorg. Chem. 43 (1998) 81.
[121] N.S. Panina, Y.N. Kukushkin, Zh. Neorg. Khim. 44 (1999) 1334; N.S. Panina, Y.N. Kukushkin, Russ. J. Inorg. Chem. 44 (1999) 1260.
[122] S.J. Stevens, H. Basch, M. Krauss, P. Jasien, Can. J. Chem. 70 (1992) 612.

[123] N.S. Panina, Y.N. Kukushkin, Zh. Neorg. Khim. 44 (1999) 798;
N.S. Panina, Y.N. Kukushkin, Russ. J. Inorg. Chem. 44 (1999) 738.
[124] Y.N. Kukushkin, V.K. Krylov, S.F. Kaplan, M. Calligaris, E. Zangrando, A.J.L. Pombeiro, V.Y. Kukushkin, Inorg. Chim. Acta 285 (1999) 116.
[125] N.S. Panina, Y.N. Kukushkin, M. Calligaris, Zh. Neorg. Khim. 45 (2000) 1005;
N.S. Panina, Y.N. Kukushkin, M. Calligaris, Russ. J. Inorg. Chem. 45 (2000) 904.
[126] N.S. Panina, M. Calligaris, Inorg. Chim. Acta 334 (2002) 165.
[127] W.J. Mortier, Struct. Bonding 66 (1987) 125;
R.T. Sanderson, J. Chem. Ed. 31 (1954) 2.
[128] M. Stener, M. Calligaris, J. Mol. Struct. (Theochem.) 497 (2000) 91.
[129] M. Calligaris, P. Faleschini, F. Todone, E. Alessio, S. Geremia, J. Chem. Soc., Dalton Trans. (1995) 1653.
[130] E. Alessio, M. Bolle, B. Milani, G. Mestroni, P. Faleschini, S. Geremia, M. Calligaris, Inorg. Chem. 34 (1995) 4716.
[131] M. Calligaris, N.S. Panina, J. Mol. Struct. 646 (2003) 61.
[132] E. Alessio, E. Iengo, S. Geremia, M. Calligaris, Inorg. Chim. Acta 344 (2003) 183.
[133] S. Geremia, M. Calligaris, J. Chem. Soc., Dalton Trans. (1997) 1541.
[134] S. Geremia, L. Vicentini, M. Calligaris, Inorg. Chem. 37 (1998) 4094.
[135] E. Alessio, E. Iengo, E. Zangrando, S. Geremia, P.A. Marzilli, M. Calligaris, Eur. J. Inorg. Chem. (2000) 2207.
[136] S. Geremia, M. Calligaris, Y.N. Kukushkin, A.V. Zinchenko, V.Y. Kukushkin, J. Mol. Struct. 516 (2000) 49.
[137] M. Iwamoto, E. Alessio, L.G. Marzilli, Inorg. Chem. 35 (1996) 2384.
[138] D.T.T. Yapp, S.J. Rettig, B.R. James, K.A. Skov, Inorg. Chem. 36 (1997) 5635.
[139] S.N. Shashkov, M.A. Kiselev, S.N. Tioutiounnikov, A.M. Kiselev, P. Lesieur, Phys. B 271 (1999) 184.
[140] T.S. Khodashova, M.A. Porai-Koshits, V.S. Sergienko, L.A. Butman, Y.A. Uslaev, V.V. Kobalev, A.A. Kutznetsova, Koord. Khim. 4 (1978) 1909.
[141] Y.N. Kukushkin, V.K. Krylov, Y.E. Larianova, Zh. Obshch. Khim. 65 (1995) 881.
[142] L.J. Bellamy, The Infra-Red Spectra of Complex Molecules, Wiley, London, 1957.
[143] S. Gama de Almeida, J.L. Hubbard, N. Farrell, Inorg. Chim. Acta 193 (1992) 149.
[144] V.K. Belsky, V.E. Konovalov, V.Y. Kukushkin, A.I. Moiseev, Inorg. Chim. Acta 169 (1990) 101.
[145] V.Y. Kukushkin, V.K. Belsky, V.E. Konovalov, G.A. Kirakosyan, L.V. Konovalov, A.I. Moiseev, V.M. Tkachuk, Inorg. Chim. Acta 185 (1991) 143.
[146] F.D. Rochon, P.C. Kong, R. Melanson, Inorg. Chem. 29 (1990) 1352.
[147] V.Y. Kukushkin, V.K. Belski, E.A. Aleksandrova, E.Y. Pankova, V.E. Konovalov, Phosphorus Sulfur Silicon 68 (1992) 253.
[148] T.A.K. Al-Allaf, L.J. Rashan, A.S. Abu-Surrah, R.andM. Steinmann, Trans. Met. Chem. 23 (1998) 403.
[149] W.I. Sundquist, K.J. Ahmed, L.S. Hollis, S.J. Lippard, Inorg. Chem. 26 (1987) 1524.
[150] G. Annibale, L. Cattalini, V. Bertolasi, V. Ferretti, G. Gilli, M.L. Tobe, J. Chem. Soc., Dalton Trans. (1989) 1265.
[151] M.J. Bennett, F.A. Cotton, D.L. Weaver, R.J. Williams, W.H. Watson, Acta Crystallogr. 23 (1967) 788.
[152] D.R. Evans, M. Huang, W.M. Seganish, J.C. Fettinger, T.L. Williams, Inorg. Chem. Commun. 6 (2003) 462.
[153] P.S.C. Cartwright, R.D. Gillard, E.R.J. Sillanpaa, J. Valkonen, Tetrahedron 7 (1988) 2143.
[154] F.A. Cotton, E.V. Dikarev, M.A. Petrukhina, S.-E. Stiriba, Inorg. Chem. 39 (2000) 1748.
[155] E. Alessio, G. Balducci, M. Calligaris, G. Costa, W.M. Attia, G. Mestroni, Inorg. Chem. 30 (1991) 609.
[156] A.R. Davies, F.W.B. Einstein, N.P. Farrell, B.R. James, R.S. McMillan, Inorg. Chem. 17 (1978) 1965.
[157] R.S. McMillan, A. Mercer, B.R. James, J. Trotter, J. Chem. Soc., Dalton Trans. (1975) 1006.
[158] M. Henn, E. Alessio, G. Mestroni, M. Calligaris, W.M. Attia, Inorg. Chim. Acta 187 (1991) 39.
[159] E. Alessio, G. Balducci, A. Lutman, G. Mestroni, M. Calligaris, W.M. Attia, Inorg. Chim. Acta 203 (1993) 205.
[160] E. Alessio, G. Mestroni, G. Nardin, W.M. Attia, M. Calligaris, G. Sava, S. Zorzet, Inorg. Chem. 27 (1988) 4099.
[161] L. Coghi, C. Pelizzi, G. Pelizzi, J. Organometal. Chem. 114 (1976) 53.
[162] P. Biscarini, L. Fusina, G.D. Nivellini, A. Mangia, G. Pelizzi, J. Chem. Soc., Dalton Trans. (1973) 159.
[163] P. Biscarini, L. Fusina, G. D. Nivellini, A. Mangia, G. Pelizzi, J. Chem. Soc., Dalton Trans. (1974) 1846.
[164] H. Schmidbaur, H.-J. Öller, S. Gamper, G. Müller, J. Organometal. Chem. 394 (1990) 757.
[165] J.T. Guy Jr., J.C. Cooper, R.D. Gilardi, J.L. Flippen-Anderson, C.F. George Jr., J. Inorg. Chem. 27 (1988) 635.
[166] M. Nonoyama, K. Nakajima, Polyhedron 18 (1999) 533.
[167] O.V. Rudnitskaya, T.M. Buslaeva, A.I. Stash, A.V. Kisin, Koord. Khim. 21 (1995) 144.
[168] J.E. Fergusson, C.T. Page, W.T. Robinson, Inorg. Chem. 15 (1976) 2270.
[169] C. Schumaker, F. Weller, K. Dehnicke, Z. Anorg. Allg. Chem. 508 (1984) 79.
[170] O.V. Rudnitskaya, I.V. Miroshnichenko, A.I. Stash, N.M. Sinitsyn, Russ. J. Inorg. Chem. 38 (1993) 1101.